Supplementary Information

Controllable DNA strand displacement by independent metal-ligand complexation

Liang-Liang Wang[a], Qiu-Long Zhang[a], Yang Wang[a], Yan Liu[a], Jiao Lin[a], Fan Xie[a] and Liang Xu*[a]

[a] *MOE Key Laboratory of Bioinorganic and Synthetic Chemistry, School of Chemistry, Sun Yat-Sen University, Guangzhou, 510275, China.*

**E-mail: xuliang33@mail.sysu.edu.cn*

Table of Contents

Materials and methods

All chemicals and solvents were commercial and used without further purification. All unmodified DNA sequences used in this study were ordered from Sangon Biotech. The DNA phosphoramidites and CPG were purchased from DNA Chem. The compound masses were weighed on a microbalance with a resolution of 0.1 mg. TLC (Thin-layer chromatography) analysis was performed through pre-coated silica gel plates. Column chromatography carried out by silica gel (#100–200). ^{1}H and ^{13}C NMR spectra were recorded on Bruker AVANCE III 400 MHz spectrometer using DMSO-d_6 as solvent, or TMS as internal standard. The chemical shifts were reported in parts per million (ppm), the coupling constants (J) were expressed in hertz unit (Hz) and signals were described as singlet (s), doublet (d), triplet (t), broad (br) as well as multiplet (m). The mass spectra (MS) were recorded on LCMS-2010A. Gel shift was imaged by Gel Image System (Tanon 2500R). The fluorescence was recorded by a SHIMADZU-RF-6000 fluorescence spectrophotometer.

Synthesis of 8HQ-phosphoramidites

Scheme S1. Synthetic route of 8HQ-nucleotides **7a–b**.

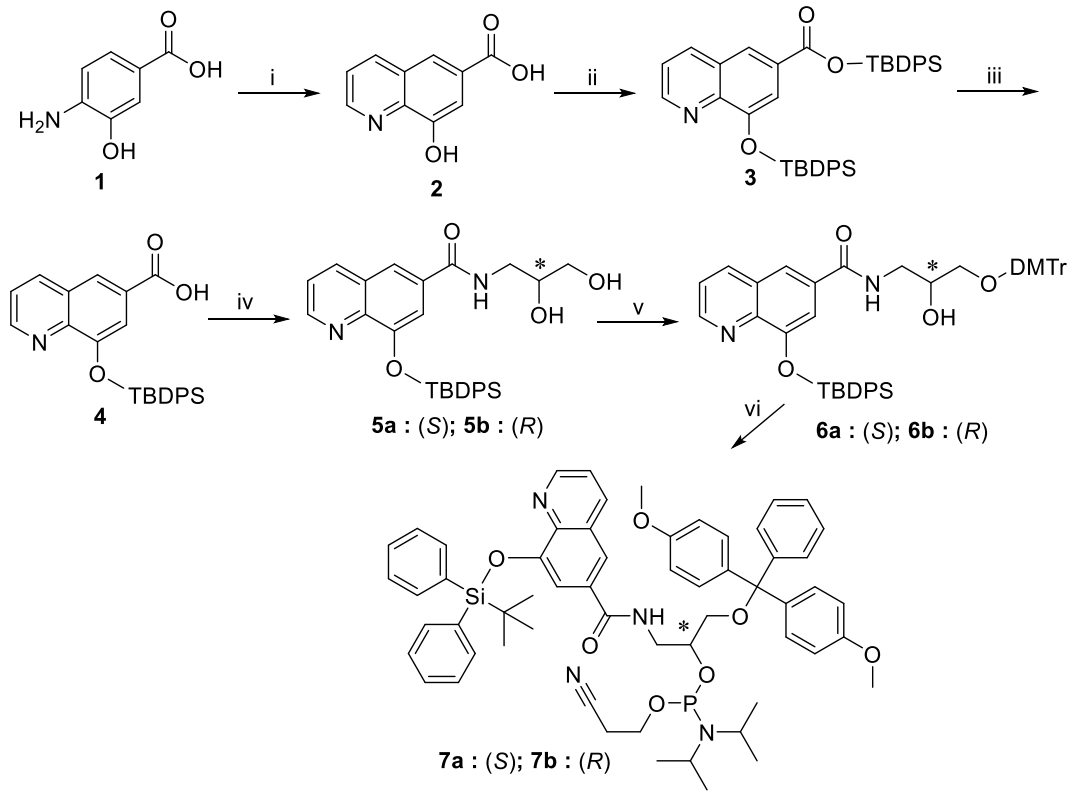

Reagents and conditions: (i) acrolein, 6 M HCl, 100 °C, 1 h, 30.9%; (ii) imidazole, tert-butyldiphenylchlorosilane, *N*, *N*-dimethylformamide, r.t., 12 h, 80.3%; (iii) acetonitrile/ammonium hydroxide (V/V) = 50/3, r.t., 4 h, 75.5%; (iv) *N*, *N*'-carbonyldiimidazole, (*S*) 3-amino-1,2-propanediol or (*R*) 3-amino-1,2-propanediol, *N*, *N*-dimethyl formamide, 0 °C, 2 h, 40.1–44.2%; (v) 4, 4'-dimethoxytrityl chloride, 4-dimethylaminopyridine, pyridine, r.t., 12 h, 33.2–39.4%; (vi) *N*, *N*-diisopropylethylamine, 2-cyanoethyl-*N*, *N*-diisopropylaminochloro phosphite, CH_2Cl_2, 0 °C, 2 h, 72.3–75.2%.

1.1 Synthesis of 8-hydroxyquinoline-6-carboxylic acid (2)

The intermediate **2** was prepared according to the previously reported procedures.[1] To a stirred suspension of 4-amino-3-hydroxybenzoic acid (2.0 g, 13.0 mmol) in 6 M HCl (40 mL) was added acrolein (7.29 g, 0.13 mol) consecutively. The mixture was stirred at 100 °C for 1 h. After the completion of reaction, it was neutralized with a saturated aqueous solution of $NaHCO_3$. The precipitate was filtered off, and then the filtrate acidified to pH 4 with HCl. The aqueous phase was extracted with EtOAc (3× 100 mL), and the organic extract was dried over anhydrous sodium sulfate and concentrated. The crude product was purified by crystallization from CH_2Cl_2 to afford corresponding **2** (0.76 g) as white solid. Yield: 30.9%; ^{1}H NMR (400 MHz, DMSO-d_6) δ 10.17 (s, 1H), 8.96 (dd, J = 4.1, 1.5 Hz, 1H), 8.51 (dd, J = 8.4, 1.4 Hz, 1H), 8.11 (d, J = 1.5 Hz, 1H), 7.63 (dd, J = 8.3, 4.2 Hz, 1H), 7.52 (d, J = 1.6 Hz, 1H) ppm; ^{13}C NMR (101 MHz, DMSO-d_6) δ 167.62, 154.02, 150.78, 140.82, 138.06, 129.91, 128.58, 122.99, 120.99, 110.91 ppm; MS (ESI) calcd. for $C_{10}H_7NO_3$ $[M + H]^+$, 190.0504; found, 190.08.

1.2 Synthesis of tert-butyldiphenylsilyl 8-((tert-butyldiphenylsilyl)oxy)quinoline-6-carboxylate (3)

To a stirred solution of intermediate **2** (0.60 g, 3.17 mmol) in dry *N*, *N*-dimethylformamide (10 mL) was added imidazole (0.54 g, 7.93 mmol) and tert-butyldiphenylchlorosilane (2.18 g, 7.93 mmol). Then the mixture was stirred at room temperature for 12 h under nitrogen. After completion of the reaction, the solvent was diluted with saturated ammonium chloride (150 mL), and then extracted with EtOAc (3× 100 mL). The organic extract was dried over anhydrous sodium sulfate and evaporated under reduced pressure. The crude product was purified *via* silica gel column chromatography (eluent, EtOAc/Petroleum ether (V/V) = 7/100) to afford compound **3** (1.69 g) as white solid. Yield: 80.3%; ^{1}H NMR (400 MHz, $CDCl_3$-d_6) δ 8.86 (s, 1H), 8.21 (s, 1H), 8.17 (d, J = 8.2 Hz, 1H), 7.82 (d, J = 7.6 Hz, 4H), 7.71 (s, 1H), 7.66 (d, J = 7.6 Hz, 4H), 7.46 (t, J = 7.3 Hz, 2H), 7.40 (s, 7H), 7.31 (t, J = 7.8 Hz, 4H), 1.26 (s, 9H), 1.05 (s, 9H) ppm; ^{13}C NMR (101 MHz, $CDCl_3$-d_6) δ 165.20, 152.30, 150.84, 137.00,

135.34, 133.35, 131.61, 130.07, 129.60, 129.12, 128.61, 127.65, 124.37, 121.90, 117.13, 26.84, 20.09, 19.12 ppm; MS (ESI) calcd. for $C_{42}H_{43}NO_3Si_2$ $[M + H]^+$, 666.2860; found, 666.48.

1.3 Synthesis of 8-((tert-butyldiphenylsilyl)oxy)quinoline-6-carboxylic acid (4)

Compound **4** (1.50 g, 2.56 mmol) was dissolved in 100 ml of a mixed solution of acetonitrile and ammonia (V/V = 50/3), and stirred at room temperature for 4 h. After the completion of reaction, the solvent was evaporated under reduced pressure and the residue was diluted with saturated ammonium chloride (150 mL), and then extracted with EtOAc (3× 100 mL). The organic extract was dried over anhydrous sodium sulfate and concentrated. The crude product was purified *via* silica gel column chromatography (eluent, EtOAc/Petroleum ether (V/V) = 30/70) to afford corresponding compound **4** (0.83 g) as white solid. Yield: 75.5%; ^{1}H NMR (400 MHz, DMSO-d_6) δ 13.05 (s, 1H), 8.82 (d, J = 2.7 Hz, 1H), 8.47 (d, J = 8.2 Hz, 1H), 8.21 (s, 1H), 7.74 (d, J = 6.8 Hz, 4H), 7.55 (dd, J = 8.2, 4.1 Hz, 1H), 7.40 (dt, J = 13.9, 4.7 Hz, 7H), 1.12 (s, 9H) ppm; ^{13}C NMR (101 MHz, DMSO-d_6) δ 167.11, 151.89, 151.46, 143.14, 137.81, 135.28, 133.31, 130.36, 129.02, 128.24, 123.95, 122.92, 116.12, 27.04, 20.05 ppm; MS (ESI) calcd. for $C_{26}H_{25}NO_3Si$ $[M + H]^+$, 428.1682; found, 428.51.

1.4 Synthesis of (S)-8-((tert-butyldiphenylsilyl)oxy)-N-(2,3-dihydroxypropyl)quinoline-6-carboxamide （5a）

To a stirred solution of compound **4** (0.75 g, 1.75 mmol) in dry *N*, *N*-dimethylformamide (10 mL) under nitrogen on an ice bath was added *N*, *N*'-carbonyldiimidazole (0.57 g, 3.50 mmol). The mixture was stirred at 0 ºC for 1 h, and then (*S*) 3-amino-1,2-propanediol (239.16 mg, 2.63 mmol) was added. The resulting mixture was continuously stirred for an additional 1 h at room temperature. After the completion of reaction, the mixture was extracted with EtOAc (3× 100 mL). The organic extract was dried over anhydrous sodium sulfate and concentrated. The crude product was purified *via* silica gel column chromatography (eluent, EtOAc/Petroleum ether (V/V) = 80/20) to afford compound **5a** (387.27 mg) as white solid. Yield: 44.2%; ^{1}H NMR (400 MHz, DMSO-d_6)) δ 8.64 (d, J = 3.8 Hz, 1H), 8.50 (t, J = 5.4 Hz, 1H), 8.32 (d, J = 8.2 Hz, 1H), 8.06 (s, 1H), 7.73 (d, J = 6.9 Hz, 4H), 7.54 (s, 1H), 7.48 (dd, J = 8.2, 4.1 Hz, 1H), 7.37 (dt, J = 13.9, 6.8 Hz, 6H), 4.80 (d, J = 4.9 Hz, 1H), 4.56 (t, J = 5.8 Hz, 1H), 3.64 (dt, J = 10.7, 5.4 Hz, 1H), 3.43–3.35 (m, 3H), 3.22–3.15 (m, 1H), 1.12 (s, 9H) ppm; ^{13}C NMR (101 MHz, DMSO-d_6) δ 166.31, 151.89, 150.29, 142.08, 137.21, 135.14, 133.91, 133.21, 130.13, 128.75, 128.10, 122.79, 120.48, 115.63, 70.82, 64.44, 43.59, 27.17, 20.14 ppm; MS (ESI) calcd. for $C_{29}H_{32}N_2O_4Si$ $[M + Na]^+$, 523.2029; found, 523.53.

1.5 Synthesis of (R)-8-((tert-butyldiphenylsilyl)oxy)-N-(2,3-dihydroxypropyl)quinoline-6-carboxamide （5b）

Compound **5b** was prepared according to the procedure described for compound **5a** starting from compound **4** (0.75 g, 1.75 mmol), *N*, *N*'-carbonyldiimidazole (0.57 g, 3.50 mmol) and (*R*) 3-amino-1,2-propanediol (239.16 mg, 2.63 mmol). The corresponding compound **5b** (315.35 mg) was obtained as white solid. Yield: 40.1%; ^{1}H NMR (400 MHz, DMSO-d_6) δ 8.64 (d, J = 2.7 Hz, 1H), 8.50 (t, J = 5.4 Hz, 1H), 8.32 (d, J = 8.1 Hz, 1H), 8.06 (s, 1H), 7.73 (d, J = 6.8 Hz, 4H), 7.54 (s, 1H), 7.48 (dd, J = 8.3, 4.1 Hz, 1H), 7.38 (dq, J = 13.9, 7.1 Hz, 6H), 4.80 (d, J = 4.9 Hz, 1H), 4.56 (t, J = 5.7 Hz, 1H), 3.64 (dt, J = 10.7, 5.4 Hz, 1H), 3.36 (d, J = 5.7 Hz, 2H), 3.22–3.15 (m, 1H), 3.12–3.06 (m, 1H), 1.12 (s, 9H) ppm; ^{13}C NMR (101 MHz, DMSO-d_6) δ 166.31, 151.89, 150.30, 142.08, 137.21, 135.14, 133.91, 133.21, 130.13, 128.75, 128.10, 122.79, 120.48, 115.63, 70.81, 64.44, 43.59, 27.17, 20.14 ppm; MS (ESI) calcd. for $C_{29}H_{32}N_2O_4Si$ $[M + Na]^+$, 523.2029; found, 523.51.

1.6 Synthesis of (S)-N-(3-(bis(4-methoxyphenyl)(phenyl)methoxy)-2-hydroxypropyl)-8-((tert-butyldiphenylsilyl)oxy)quinoline-6-carboxamide (6a)

To a stirred solution of compound **5a** (0.30 g, 0.60 mmol) in dry pyridine (5 mL) was added 4, 4'-dimethoxytrityl chloride (406.59 g, 1.20 mmol) and 4-dimethylaminopyridine (7.33 mg, 0.06 mmol). The mixture was stirred at room temperature for 12 h under nitrogen. After the completion of reaction, the solvent was evaporated under reduced pressure and the residue was purified *via* silica gel column chromatography (eluent, CH_2Cl_2/Petroleum ether (V/V) = 40/60) to give the desired product **6a** (189.83 mg) as white solid. Yield: 39.4%; ^{1}H NMR (400 MHz, DMSO-d_6) δ 8.64 (d, J = 2.7 Hz, 1H), 8.43 (t, J = 4.9 Hz, 1H), 8.29 (d, J = 7.9 Hz, 1H), 7.97 (s, 1H), 7.73 (d, J = 6.8 Hz, 4H), 7.54 (s, 1H), 7.48 (dd, J = 8.2, 4.1 Hz, 1H), 7.38 (dt, J = 14.2, 7.5 Hz, 8H), 7.27 (d, J = 7.9 Hz, 6H), 7.18 (t, J = 7.2 Hz, 1H), 6.84 (dd, J = 8.5, 4.1 Hz, 4H), 5.05 (d, J = 5.3 Hz, 1H), 3.88 (dt, J = 10.9, 5.3 Hz, 1H), 3.67 (d, J = 4.9 Hz, 6H), 3.51–3.44 (m, 1H), 3.25–3.17 (m, 1H), 2.97 (p, J = 9.4 Hz, 2H), 1.12 (s, 9H) ppm; ^{13}C NMR (101 MHz, DMSO-d_6) δ 166.10, 158.44, 151.88, 150.26, 145.52, 142.06, 137.16, 136.29, 135.12, 133.95, 133.22, 130.15, 128.70, 128.53–127.98, 126.98, 122.77, 120.42, 115.63, 113.53, 85.70, 68.96, 66.40, 55.39, 44.02, 27.18, 20.15 ppm; MS (ESI) calcd. for $C_{50}H_{50}N_2O_6Si$ $[M + H]^+$, 803.3516; found, 803.60.

1.7 Synthesis of (R)-N-(3-(bis(4-methoxyphenyl)(phenyl)methoxy)-2-hydroxypropyl)-8-((tert-butyldiphenylsilyl)oxy)quinoline-6-carboxamide (6b)

Compound **6b** was prepared according to the procedure described for compound **6a** starting from compound **5b** (0.30 g, 0.60 mmol), 4, 4'-dimethoxytrityl chloride (406.59 g, 1.20 mmol)

and 4-dimethylaminopyridine (7.33 mg, 0.06 mmol). The corresponding compound **6b** (159.96 mg) was obtained as white solid. Yield: 33.2%; ^{1}H NMR (400 MHz, DMSO-d_6) δ 8.64 (d, J = 2.8 Hz, 1H), 8.43 (s, 1H), 8.29 (d, J = 8.2 Hz, 1H), 7.97 (s, 1H), 7.73 (d, J = 6.9 Hz, 4H), 7.54 (s, 1H), 7.48 (dd, J = 8.2, 4.1 Hz, 1H), 7.38 (dt, J = 14.2, 7.6 Hz, 8H), 7.27 (d, J = 8.2 Hz, 6H), 7.19 (d, J = 7.2 Hz, 1H), 6.84 (dd, J = 8.5, 4.1 Hz, 4H), 5.05 (d, J = 5.2 Hz, 1H), 3.92–3.85 (m, 1H), 3.67 (d, J = 4.9 Hz, 6H), 3.51–3.44 (m, 1H), 3.25–3.17 (m, 1H), 2.97 (p, J = 9.4 Hz, 2H), 1.12 (s, 9H) ppm; ^{13}C NMR (101 MHz, DMSO-d_6) δ 166.10, 158.44, 151.88, 150.26, 145.52, 142.06, 137.16, 136.29, 135.11, 133.95, 133.22, 128.70, 128.44–127.98, 126.98, 122.77, 120.42, 115.63, 113.53, 85.70, 68.96, 66.40, 55.39, 44.02, 27.18, 20.15 ppm; MS (ESI) calcd. for $C_{50}H_{50}N_2O_6Si$ $[M + H]^+$, 803.3516; found, 803.51.

1.8 Synthesis of (S)-1-(bis(4-methoxyphenyl)(phenyl)methoxy)-3-(8-((tert-butyldiphenylsilyl) oxy)quinoline-6-carboxamido)propan-2-yl (2-cyanoethyl) diisopropylphosphoramidite (7a)

To a stirred solution of compound **6a** (0.17 g, 0.21 mmol) in anhydrous CH_2Cl_2 (5 mL) was added *N*, *N*-diisopropylethylamine (109.74 μL, 0.63 mmol) and 2-cyanoethyl-*N*, *N*-diisopropylaminochlorophosphite (93.69 μL, 0.42 mmol). The mixture was stirred on an ice bath under nitrogen for 2 h. After the completion of reaction, the solvent was evaporated under reduced pressure and the residue was purified *via* silica gel column chromatography (eluent, 1% TEA, EtOAc/Petroleum ether (V/V) = 20/80) to give the target product **7a** (152.36 mg) as white solid. Yield: 72.3%; ^{1}H NMR (400 MHz, DMSO-d_6) δ 8.61 (s, 1H), 8.57–8.46 (m, 1H), 8.27 (t, J = 7.2 Hz, 1H), 7.90 (s, 1H), 7.72 (d, J = 6.7 Hz, 4H), 7.53 (s, 1H), 7.49–7.45 (m, 1H), 7.43–7.32 (m, 8H), 7.29–7.24 (m, 6H), 7.17 (t, J = 7.2 Hz, 1H), 6.83 (dd, J = 7.4, 4.8 Hz, 4H), 4.20 (s, 1H), 3.75 (dt, J = 12.6, 6.3 Hz, 1H), 3.65 (t, J = 6.8 Hz, 7H), 3.54 (dd, J = 12.7, 6.3 Hz, 2H), 3.49–3.34 (m, 2H), 3.21–3.01 (m, 2H), 2.64 (dt, J = 11.9, 5.7 Hz, 2H), 1.11 (s, 15H), 1.07 (d, J = 6.7 Hz, 3H), 1.00 (d, J = 6.6 Hz, 3H) ppm; ^{13}C NMR (101 MHz, DMSO-d_6) δ 166.08, 158.47, 151.88, 150.18, 145.33, 142.01, 137.07, 136.08, 135.07, 134.05, 133.23, 130.11, 128.62, 128.10, 127.04, 122.79, 120.39, 119.26, 115.57, 113.52, 85.89, 72.05, 71.68, 65.09, 58.67, 55.37, 42.99, 27.18 (s), 25.03–24.29, 20.16 ppm; ^{31}P NMR (162 MHz, DMSO-d_6) δ 148.01 ppm; MS (ESI) calcd. for $C_{59}H_{67}N_4O_7PSi$ $[M + H]^+$, 1003.4595; found, 1003.67.

1.9 Synthesis of (R)-1-(bis(4-methoxyphenyl)(phenyl)methoxy)-3-(8-((tert-butyldiphenyl silyl)oxy)quinoline-6-carboxamido)propan-2-yl (2-cyanoethyl) diisopropylphosphoramidite (7b)

Compound **7b** was prepared according to the procedure described for compound **7a** starting from compound **6b** (0.14 g, 0.17 mmol), *N*, *N*-diisopropylethylamine (88.84 μL, 0.51 mmol)

and 2-cyanoethyl-*N*, *N*-diisopropylaminochlorophosphite (75.84 μL, 0.34 mmol). The corresponding target compound **7b** (128.22 mg) was obtained as white solid. Yield: 75.2%; ^{1}H NMR (400 MHz, DMSO-d_6) δ 8.61 (s, 1H), 8.57–8.45 (m, 1H), 8.27 (t, J = 7.2 Hz, 1H), 7.72 (d, J = 7.0 Hz, 4H), 7.53 (s, 1H), 7.50–7.45 (m, 1H), 7.43–7.31 (m, 8H), 7.27 (d, J = 5.7 Hz, 6H), 7.17 (t, J = 7.2 Hz, 1H), 6.85–6.78 (m, 4H), 4.20 (d, J = 5.0 Hz, 1H), 3.74 (dd, J = 14.7, 8.5 Hz, 1H), 3.69–3.66 (m, 1H), 3.64 (d, J = 3.8 Hz, 6H), 3.60–3.51 (m, 2H), 3.51–3.34 (m, 2H), 3.21–3.00 (m, 2H), 2.64 (dt, J = 11.9, 5.8 Hz, 2H), 1.11 (s, 15H), 1.07 (d, J = 6.7 Hz, 3H), 1.00 (d, J = 6.7 Hz, 3H) ppm; ^{13}C NMR (101 MHz, DMSO-d_6) δ 166.04, 158.47, 151.94, 150.19, 145.30, 142.01, 137.12, 136.12, 135.07, 134.03, 133.27, 130.17, 128.67, 128.10, 127.04, 122.79, 120.32, 119.30, 115.55, 113.53, 85.85, 72.08, 65.06, 60.34–60.14, 58.90, 58.67, 55.37, 42.93, 27.18, 25.03–24.47, 20.16 ppm;^{31}P NMR (162 MHz, DMSO-d_6) δ 148.43 ppm; MS (ESI) calcd. for $C_{59}H_{67}N_4O_7PSi$ $[M + H]^+$, 1003.4595; found, 1003.67.

Synthesis of 8HQ-modified DNA sequences

All 8HQ-containing DNA strands used in this study were chemically synthesized through the conventional phosphoramidite method by a K&A H-8 DNA Synthesizer using universal CPG as the solid phase support. After the standard procedure for DNA synthesis, the DNA products were cleaved from CPG and treated with ammonium hydroxide (22%) solution at 55 °C for 12 h to remove the protecting group. After ethanol precipitation, the crude oligonucleotides were purified by HPLC. It was performed on the Agilent 1260 system using the PLRP-S column (250 mm × 4.6 mm, 100Å, 5 μm). The mobile phase was 0.1 M TEAA (triethylammonium acetate) with 50% CH_3CN as buffer A and 0.1 M TEAA as buffer B. The oligonucleotides were purified using a gradient of 5–60% buffer A over 50 mins at a flow rate of 1 mL/min. The purified product was then lyophilized and desalted by the Bio-Spin 6 column (Bio-Rad), and stocked in TEPC-treated water at -80 °C for following experiments.

Gel shift assay for measurements of DNA strand displacement

An stock of duplex 1 (S_L : $\overline{S}_F$ = 1.5 : 1) was prepared by annealing (95 °C → 4 °C, 1.0 °C min^{-1}) in a reaction buffer (20 mM Tris-HCl, 100 mM NaCl; pH 7.5). An excess of S_L strand ensured efficient binding of the FAM-labeled strand ($\overline{S}_F$). The reactions were initiated by the addition of competing strand ($\overline{S}_L$) in the presence of various divalent metal ions (M^{2+}: Mg^{2+},

Ca^{2+}, Mn^{2+}, Ni^{2+}, Cu^{2+}, Zn^{2+}, Pb^{2+}). It was needed to mention that the sample was treated with 10 μM EDTA before the reaction started. The purpose of this treatment was to remove the possible effect of any undesired metal ions in the buffer, given that even a nanomolar concentration of the undesired metal ion might affect the performance of this reaction. The final concentrations were: $\bar{S}_F$ = 0.5 μM, S_L = 0.75 μM, $\bar{S}_L$ = 1 μM and [M^{2+}] = 1.0 μM (the effective concentration, 10 μM EDTA + 11 μM M^{2+}) or 0 μM (treated by 1 mM EDTA). After incubated at 25 °C for 1 h, the reaction was analyzed by electrophoresis in a 15% native polyacrylamide gel on ice, and imaged by Gel Image System (Tanon 2500R). Only the fluorophore labeled strand was visualized in the gel shift. For the time-dependent analysis, aliquots of the above reaction samples were quenched by addition of (1 mM) EDTA at the designated time points, and analyzed as described above.

For pH-dependent kinetic analysis, all the conditions remained the same except the pH values of the reaction buffer. For metal concentration-dependent kinetic analysis, all the conditions remained the same except the concentration of the copper ion. After incubation at 25 °C for different time points, these reaction samples were quenched by treatment of 1 mM EDTA for the native PAGE analysis.

Measurements of the duplex melting temperatures

The solutions for the thermal denaturation studies contained a 1:1 ratio of two complementary DNA strands. The final concentrations of DNA strand and metal ions were: the duplex ($S_{L\text{-}Q}$: $\bar{S}_{L\text{-}F}$ (***S***), $S_{L\text{-}Q}$: $\bar{S}_{L\text{-}F}$ (***R***), S_Q : $\bar{S}_F$ or $S_{Q\text{-}T}$: $\bar{S}_{F\text{-}A}$) = 0.5 μM and [M^{2+}] = 1.0 μM (effective concentration, 10 μM EDTA + 11 μM M^{2+}) or 0 μM (in the presence of 1 mM EDTA). The sample was pre-treated with 10 μM EDTA to remove the possible effect of any undesired metal ions in the buffer as described above. The mixture solution was firstly annealed (95 °C → 4 °C, 1.0 °C min^{-1}) in a reaction buffer (20 mM sodium cacodylate with pH 7.5 and 100 mM NaCl) to form the duplex structure. The fluorescence was then recorded by the Bio-Rad CFX96 Touch real-time fluorescence quantitative PCR (λ_{ex} = 480 nm, λ_{em} = 520 nm) along with the increasing temperature from 4 to 95 °C. The heating rate was 1.0 °C min^{-1}. To calculate the melting temperature (T_m), the change of fluorescence intensity was normalized, and the T_m values were determined by the temperature with 50% change of fluorescence at

520 nm.

Kinetic measurements of metal-mediated DNA strand displacement by fluorescence

An stock of duplex ($S_{L\text{-}Q}$: $\overline{S}_F$ = 1.5 : 1) was prepared by annealing (95 °C → 4 °C, 1.0 °C min^{-1}) in the reaction buffer (20 mM Tris-HCl with pH 7.5 and 100 mM NaCl). An excess of $S_{L\text{-}Q}$ strand was added to ensure efficient binding of the FAM-labeled strand ($\overline{S}_F$). The reaction was started by the addition of competing strand ($\overline{S}_L$) and the copper ion. The final concentrations of DNA strands and the metal ion were: $\overline{S}_F$ = 0.5 μM, $S_{L\text{-}Q}$ = 0.75 μM, $\overline{S}_L$ = 1 μM and the designated concentration of Cu^{2+}. All the modified ligands in the kinetic experiments were the *S*-configuration, unless otherwise stated. It was needed to mention that the sample was pre-treated with 100 nM EDTA when the concentration of copper ion was in the nanomolar level. The purpose of this treatment was to remove the possible effect of any undesired metal ions in the buffer, as even a nanomolar concentration of the undesired metal ion might affect the performance of this reaction when the concentration of copper ion was very low. The fluorescence kinetics was monitored by a SHIMADZU-RF-6000 fluorescence spectrophotometer (λ_{ex} = 480 nm, λ_{em} = 520 nm, Time interval: 1 s).

For the fluorescence kinetic measurement of conventional toehold-mediated DNA strand displacement (Figure 4a in the main text), same conditions were adopted with the corresponding strands ($\overline{S}_F$ = 0.5 μM, $S_{T\text{-}Q}$ = 0.75 μM, $\overline{S}_T$ = 1 μM).

For the kinetic comparison in the presence of a high concentration (10×) of unmodified competing strand ($\overline{S}_1$) (Figure 4b in the main text), the annealed duplex ($S_{L\text{-}Q}$: $\overline{S}_F$) and 10-eq $\overline{S}_1$ were premixed before addition of $\overline{S}_L$ and Cu^{2+} to trigger the reaction. The final concentrations for all these strands were 0.5 μM ($\overline{S}_F$), 0.75 μM ($S_{L\text{-}Q}$), 1 μM ($\overline{S}_L$), 10 μM ($\overline{S}_1$).

For the kinetic comparison when the ligand-modified competing strand ($\overline{S}_L$) was masked by the complementary sequence (S_1) (Figure 4c in the main text), other conditions remained the same as described above except the competing strand ($\overline{S}_L$) was replaced by the pre-annealed duplex (S_1 : $\overline{S}_L$ = 1.2 : 1).

For the kinetic comparison when the ligand-modified competing strand ($\overline{S}_L$) was not fully matched with the strand S_L (Figure 4d in the main text), the competing strand ($\overline{S}_L$) was

replaced by the ligand-modified DNA strands with one single base mismatch at different positions ($\overline{S}_{LP1}$, $\overline{S}_{LP4}$, $\overline{S}_{LP11}$ and $\overline{S}_{LP18}$), respectively.

Measurements of the reversible strand displacement

Two types of reporter systems were introduced to monitor this process. One was unidirectional reporter systems Reporter 1 ($R1_Q$: $\overline{R1}_F$ or R1 : $\overline{R1}_F$, the latter one had the same sequence except the quenching group was absent in the R1 strand), in which the equilibrium would be shifted towards the forward direction (described in Figure 5b and 5c in the main text); the other one was a bidirectional reporter system Reporter 2 ($R2_Q$: $\overline{R2}_F$), in which the reporting signals were altered based on the shift of the seesaw system (described in Figure 5d in the main text). The reporter systems and the initial duplex (S_{LT} : $\overline{S}_{T1}$) were prepared by annealing (95 °C → 4 °C, 1.0 °C min^{-1}) in a reaction buffer (20 mM Tris-HCl, 100 mM NaCl; pH 8.0).

For the fluorescence measurements of the unidirectional reporter system monitored the toehold exchange (Figure 5b), the initial duplex (S_{LT} and $\overline{S}_{T1}$) and Reporter 1 ($R1_Q$: $\overline{R1}_F$) were mixed in the presence or absence of copper ions before the addition of the input strand $\overline{S}_L$ to start the reaction. The fluorescence change was monitored by real-time fluorescence analysis. The final concentrations of DNA strands and the copper ion were: $\overline{R1}_F$ = 0.5 μM, $R1_Q$ = 0.6 μM, $\overline{S}_{T1}$ = 0.65 μM, S_{LT} = 0.78 μM, $\overline{S}_L$ = 0.975 μM and $[Cu^{2+}]$ = 1.0 μM or 0 μM. The reaction buffer was 20 mM Tris-HCl (pH = 8.0) with 100 mM NaCl. For the absence of copper ions, 1 mM EDTA was added into the reaction buffer.

For the gel-based assays using the unidirectional reporter system (Figure 5c and S12), the pre-annealed duplex DNA (S_{LT} and $\overline{S}_{T1}$) and the competing strand $\overline{S}_L$ were mixed before addition of Cu^{2+} as the first step (State A). One aliquot of this sample was then reacted with Reporter 1 ($R1_Q$: $\overline{R1}_F$ or R1 : $\overline{R1}_F$). The sample was then incubated with 1 μM Cu^{2+} for 40 min (State B), and another aliquot of this sample was reacted with Reporter 1 thereafter. The rest sample was further treated with 1 mM EDTA for 40 min to break the metal-ligand coordination (Back to State A), and followed by the reaction with Reporter 1 (R1 : $\overline{R1}_F$). The reactions with Reporter 1 ($R1_Q$: $\overline{R1}_F$) were monitored by the kinetic mode of fluorescence.

All reactions with Reporter 1 (R1 : $\overline{R1}_F$ without the quenching group) were performed at room temperature for over 30 min to ensure the reporting procedure to proceed totally before gel analysis. The final concentrations of these DNA strands were: $\overline{R1}_F$ = 0.5 μM, R1 or $R1_Q$ = 0.6 μM, $\bar{S}_{T1}$ = 0.65 μM, S_{LT} = 0.78 μM and $\bar{S}_L$ = 0.975 μM. The reaction buffer was 20 mM Tris-HCl (pH = 8.0) with 100 mM NaCl.

For the reversible control of toehold exchange by the bidirectional reporter system (Figure 5d and Figure S13), the samples were prepared by mixing the pre-annealed duplex (S_{LT} : $\bar{S}_{T1}$), Reporter 2 ($R2_Q$: $\overline{R2}_F$) and input strand ($\bar{S}_L$) in a reaction buffer (20 mM Tris-HCl, 100 mM NaCl; pH 8.0). The final concentrations of these strands were: $\overline{R2}_F$ = 0.5 μM, $R2_Q$ = 0.6 μM, $\bar{S}_{T1}$ = 0.65 μM, S_{LT} = 0.78 μM and $\bar{S}_L$ = 0.975 μM. The fluorescence of the initial sate without treatment of Cu^{2+} was measured as "0". After treatment of 1 μM Cu^{2+}, the reaction was incubated for 40-minut to reach the equilibrium, and the fluorescence was measured as Cu^{2+}-1. Thereafter, EDTA (25 μM) was added into the mixture for another 40-minut incubation, and the fluorescence was then measured as EDTA-1. The following cyclic treatments were continued by sequential addition of 25 μM (Cu^{2+}), 50 μM (EDTA), 50 μM (Cu^{2+}), and 50 μM (EDTA). After each treatment, the reaction mixture was incubated for 40-minut to reach the equilibrium before the measurement of fluorescence (Cu^{2+}-2, EDTA-2, Cu^{2+}-3 and EDTA-3, respectively). For the conventional toehold-mediated strand displacement system (Figure S15), the sample was processed through the identical procedure except that no ligand modified DNA strand was involved. The final concentrations of DNA strands were: $\overline{R2}_F$ = 0.5 μM, $R2_Q$ = 0.6 μM, $\bar{S}_{T1}$ = 0.65 μM, S_{T2} = 0.78 μM and $\bar{S}_T$ = 0.975 μM.

For the kinetic behavior of reversible control by the bidirectional reporter system (Figure S14), other conditions remained unchanged as described in Figure 5d, only the reaction was monitored by real-time fluorescence after the sample was treated by Cu^{2+} or EDTA.

Supplementary Figures

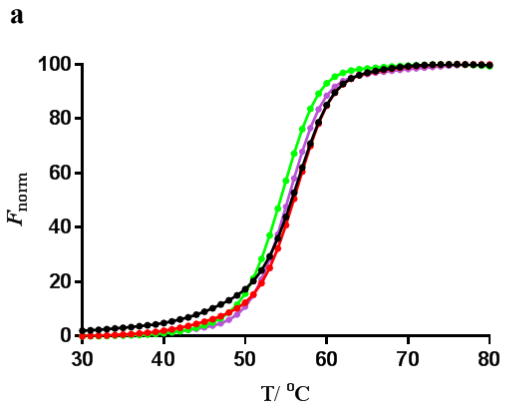

b

Duplex	T_m without Cu^{2+}
HQ-HQ (R)	55.8±0.1
HQ-HQ (S)	55.5±0.2
With A:T	55.2±0.2
Control	54.2±0.1

Figure S1. Measurements of melting temperatures (T_m) of duplex DNA in the absence of metal ions. (**a**) Melting curves of duplexes with different base pairs at termina site; (**b**) T_m values calculated from the FRET-based assays. The concentration of the duplex was 0.5 μM. 1 mM EDTA was added into the reaction buffer before the measurement. Compared with the control duplex, introduction of the HQ-HQ base pair increased the thermostability of the modified duplex DNA. Interestingly, the thermostability with the HQ-HQ base pair was even slightly stronger than the duplex with an extra A:T pair at the end, suggesting contribution of the HQ-HQ base pair was fully comparable to the natural base pair with two hydrogen bonds.

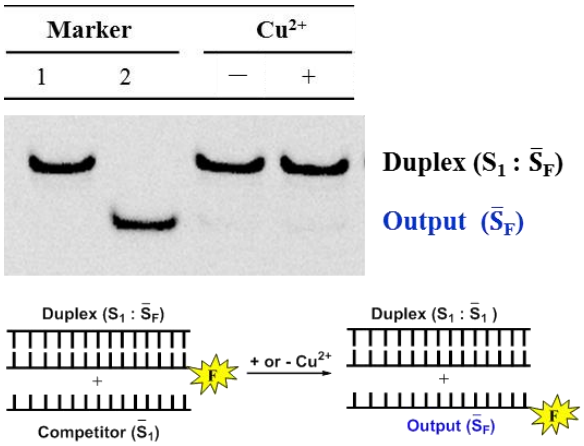

Figure S2. The direct strand displacement with unmodified DNA strands in the presence and absence of Cu^{2+}. The fluorophore-labeled strand was denoted by $\bar{S}_F$; S_1 indicated the unmodified strand that preformed a duplex structure (duplex (S_1: $\bar{S}_F$)) with the $\bar{S}_F$ strand; the competing strand (the input strand) during strand invasion was denoted by $\bar{S}_1$. Concentrations for these strands were 0.5 μM ($\bar{S}_F$), 0.75 μM (S_1) and 1 μM ($\bar{S}_1$). The reaction buffer was 20 mM Tris-HCl (pH = 7.5) with 100 mM NaCl. The effective concentration of copper ion was 1 μM; for the absence of metal ions, 1 mM EDTA was added into the reaction buffer. Native PAGE was performed after 1-hour incubation. Only the fluorophore labeled strand was visualized in the gel shift. The upper bands indicated the original duplex DNA without strand invasion (duplex (S_1: $\bar{S}_F$)). The lower bands indicated the output single stranded DNA that was displaced from the duplex (S_1: $\bar{S}_F$).

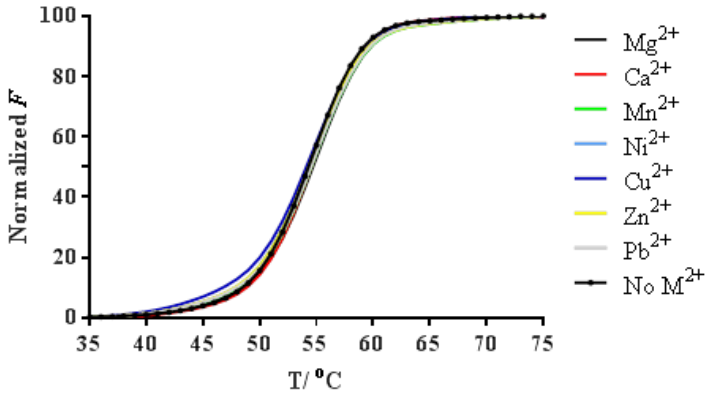

Figure S3. Measurements of melting temperatures (T_m) of unmodified duplex DNA (S_Q : $\bar{S}_F$) in the presence of different metal ions. The T_m was calculated from the FRET-based assay. The concentration of the ligand-modified duplex was 0.5 μM. Effective concentrations of divalent metal ions were 1 μM; for the absence of metal ions, 1 mM EDTA was added into the reaction buffer before the measurement.

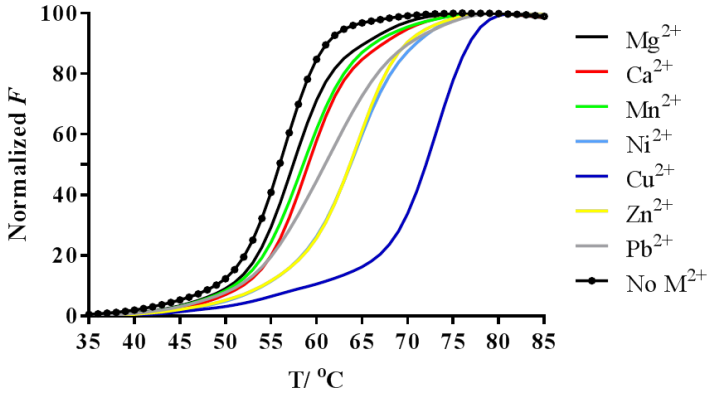

Figure S4. Measurements of melting temperatures (T_m) of ligand modified duplex DNA ($S_{L\text{-}Q}$: $\bar{S}_{L\text{-}F}$)(***S*** configuration) in the presence of different metal ions. The T_m was calculated from the FRET-based assay. The concentration of the ligand-modified duplex was 0.5 μM. Effective concentrations of divalent metal ions were 1 μM; for the absence of metal ions, 1 mM EDTA was added into the reaction buffer before the measurement.

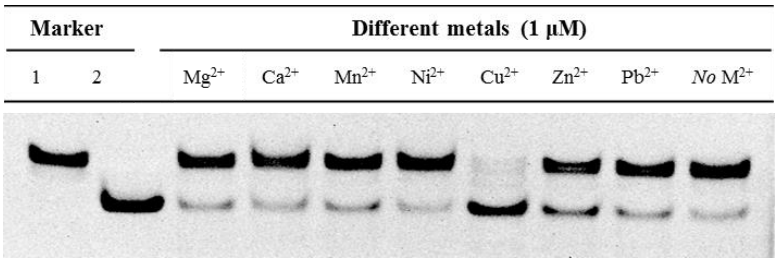

Figure S5. DNA strand invasion by coordination between the copper ion and the 8-hydroxyquinoline ligand (***S*** configuration). The gel-based results were determined by the generation of the displaced single stranded DNA (the output strand $\overline{S}_F$) as described in Figure 2b.

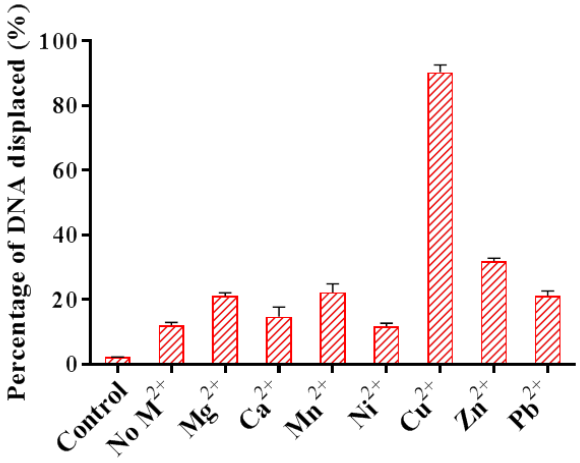

Figure S6. Quantitative comparison of the percentages of strand invasion (***S*** configuration). The control sample indicated the direct invasion without ligand modification. Error bars were derived from at least three independent replicates.

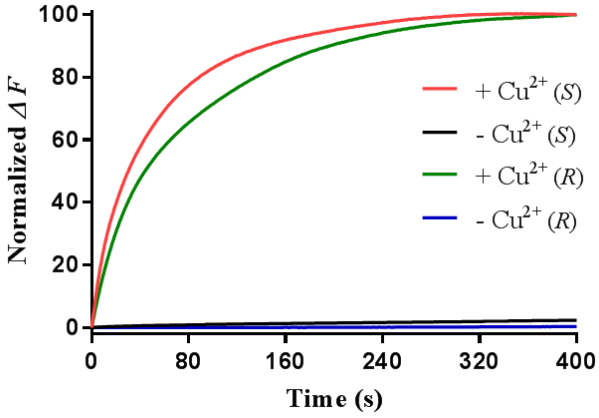

Figure S7. Measurements of kinetic behaviors using two enantiomers of HQs. Concentrations for these strands were 0.5 μM ($\overline{S}_F$), 0.75 μM ($S_{L\text{-}Q}$) and 1 μM ($\overline{S}_L$). The concentration of copper ion was 1 μM. The same strands without any divalent metal ions (with presence of 1 mM EDTA) were monitored as control. The reaction buffer was 20 mM Tris-HCl (pH = 7.5) with 100 mM NaCl. These results suggested both enantiomers exhibited similar kinetic behaviors and the chiral center has limited effects on the strand displacement.

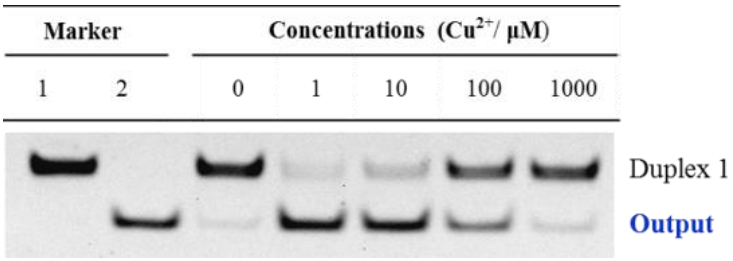

Figure S8. DNA strand invasion by coordination between different concentrations of copper ion and the 8-hydroxyquinoline ligand. The gel-based results were determined by the generation of the displaced single stranded DNA (the output strand $\overline{S}_F$) as described in Figure 2b. The concentrations of copper ions were 0, 1, 10, 100 and 1000 μM, respectively.

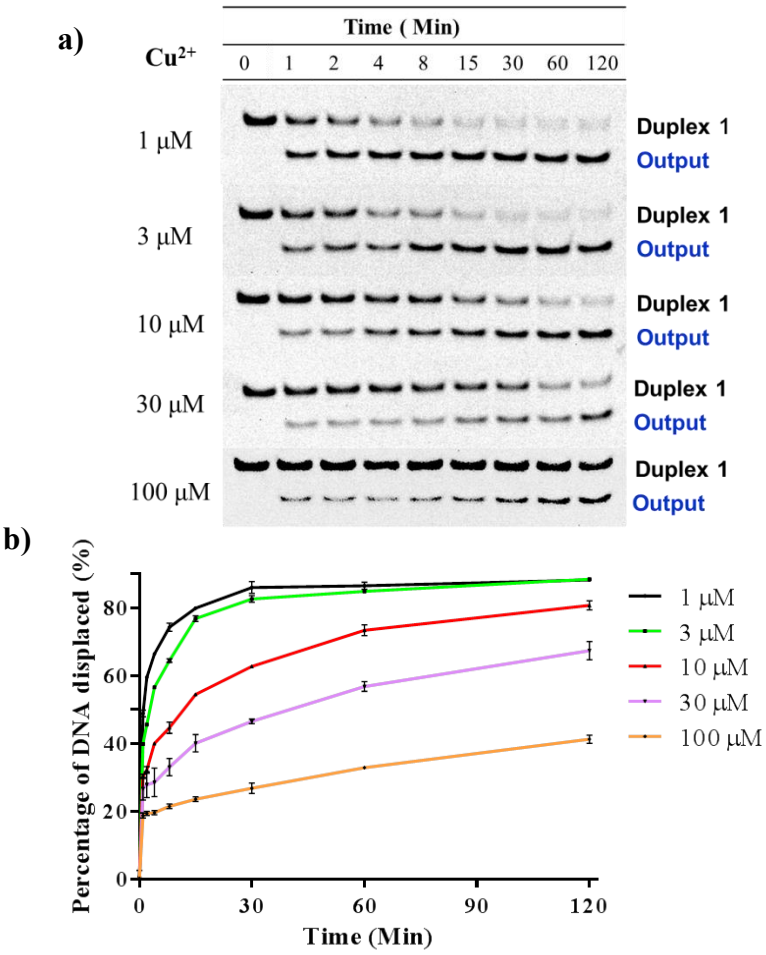

Figure S9. Concentration-dependent kinetic behaviors of metal-ligand complexation-mediated strand displacement reactions. (**a**) Concentration-dependent alterations of HQ-Cu^{2+}-HQ complexation triggered strand displacement reactions. The gel-based results were determined by the generation of the displaced single stranded DNA (the output strand $\bar{S}_F$) as described in Figure 2b. (**b**) Quantitative comparison of concentration-dependent strand displacement reactions. The concentrations of copper ions were 1, 3, 10, 30 and 100 μM, respectively. Error bars were derived from at least three independent replicates.

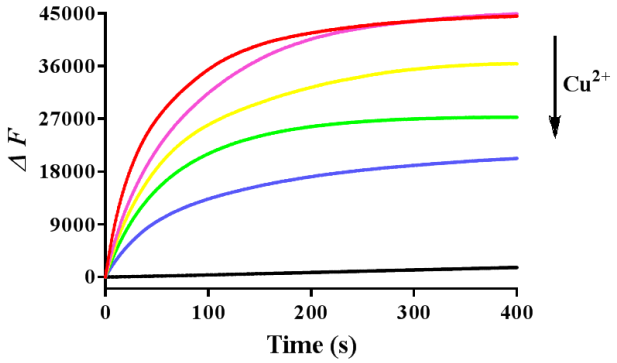

Figure S10. Measurements of sub-stoichiometric kinetic behaviors controlled by the copper ion through the increasing fluorescence of the FAM fluorophore based on the design described in Figure 3b. Concentrations for these strands were 0.5 μM ($\bar{S}_F$), 0.75 μM ($S_{L\text{-}Q}$) and 1 μM ($\bar{S}_L$). The reaction buffer was 20 mM Tris-HCl (pH = 7.5) with 100 mM NaCl and 100 nM EDTA. The concentrations of copper ions were 1100, 600, 300, 200, 150 and 0 nM, respectively.

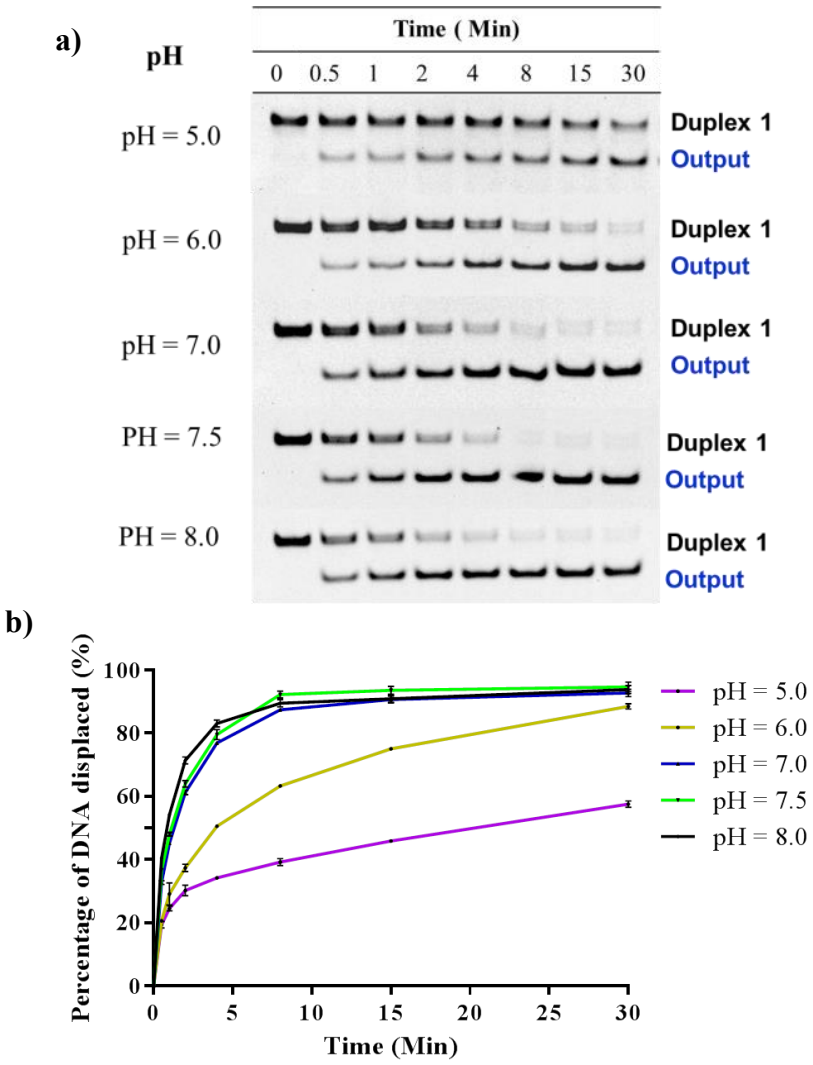

Figure S11. pH-dependent kinetic behaviors of metal-ligand complexation-mediated strand displacement reactions. (**a**) pH-dependent alterations of HQ-Cu^{2+}-HQ complexation triggered strand displacement reactions. The gel-based results were determined by the generation of the displaced single stranded DNA (the output strand $\overline{S}_F$) as described in Figure 2b. (**b**) Quantitative comparison of pH-dependent strand displacement reactions. The pH values of the reaction buffer (20 mM Tris-HCl) were 5, 6, 7, 7.5 and 8, respectively. Error bars were derived from at least three independent replicates.

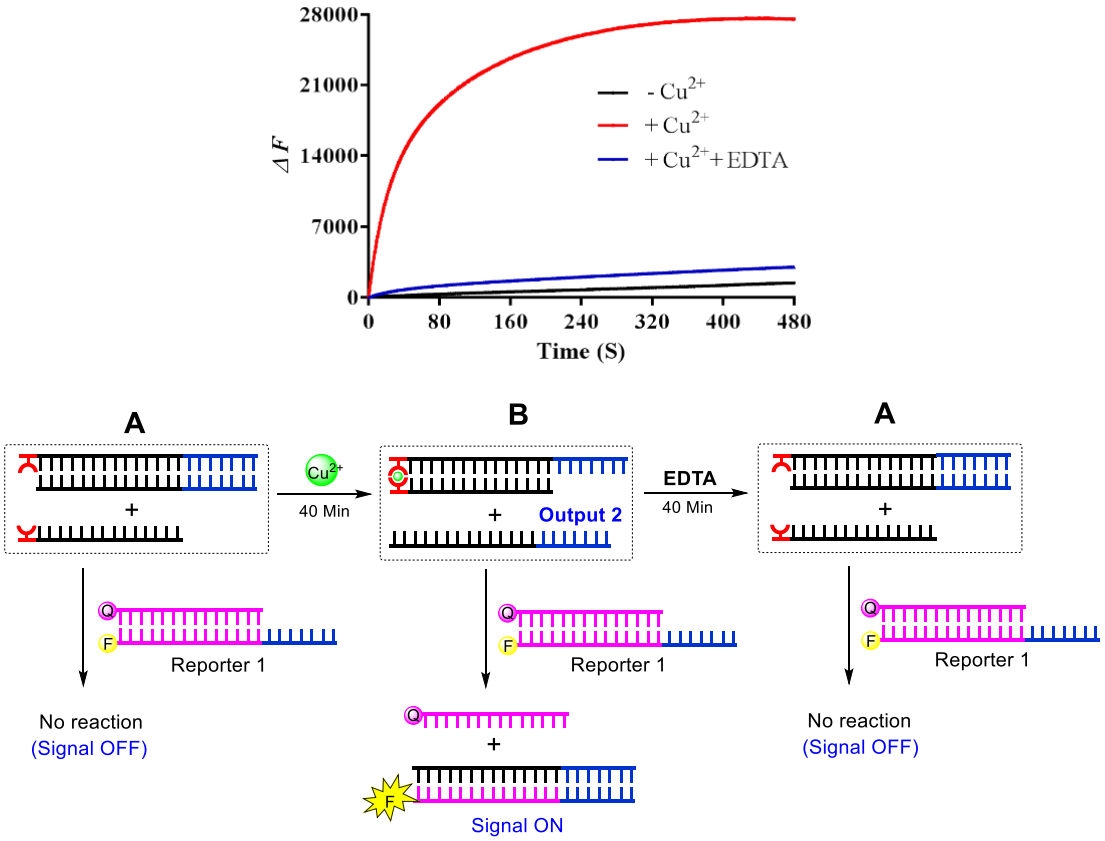

Figure S12. Monitoring the controllable reversibility by the unidirectional reporter system from the fluorescence measurements. In the absence of copper ion, State A was the stable form (the duplex formed by S_{LT} and $\overline{S}_{T1}$, and the single strand $\overline{S}_{L}$) without the release of the output strand ($\overline{S}_{T1}$), and as a result, the unidirectional reporter system ($R1_{Q}$ and $\overline{R1}_{F}$) could not report any strand displacement reaction (black curve). After the addition of copper ion, the State B could be generated with the release of output strand, and therefore, the reporting signal could be monitored from fluorescence. Once EDTA was mixed together after incubation of Cu^{2+}, the released output strand would invade the newly-formed duplex and make the state B change back to A again. Therefore, the reporter duplex was unable to detect the significant release of the output strand.

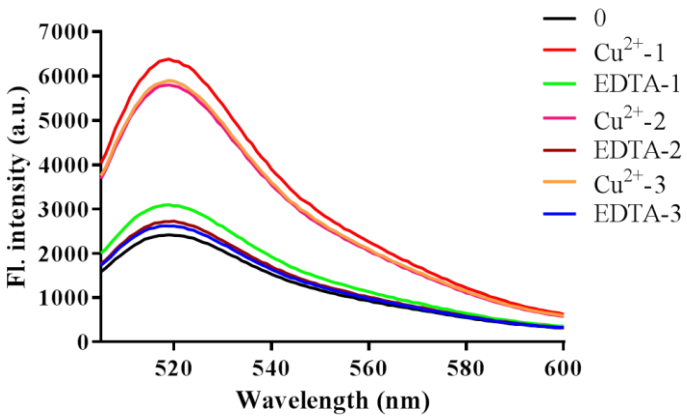

Figure S13. Fluorescence spectra of the reversible control of toehold exchange by the bidirectional reporter system. In the bidirectional reporter system ($R2_Q$ and $\overline{R2}_F$), the controllable reversibility was governed by the metal-ligand complexation between State A and B. In the first cycle, the addition of copper ion was 1 μM and the addition of EDTA was 25 μM; in the second cycle, the addition of copper ion was 25 μM and the addition of EDTA was 50 μM; in the third cycle, the addition of copper ion was 50 μM and the addition of EDTA was 50 μM. After each treatment, the reaction mixture was incubated for 40-minut to reach the equilibrium before the measurement of fluorescence. Concentrations for all these strands were described in the methods. The reaction buffer was 20 mM Tris-HCl (pH = 8.0) with 100 mM NaCl.

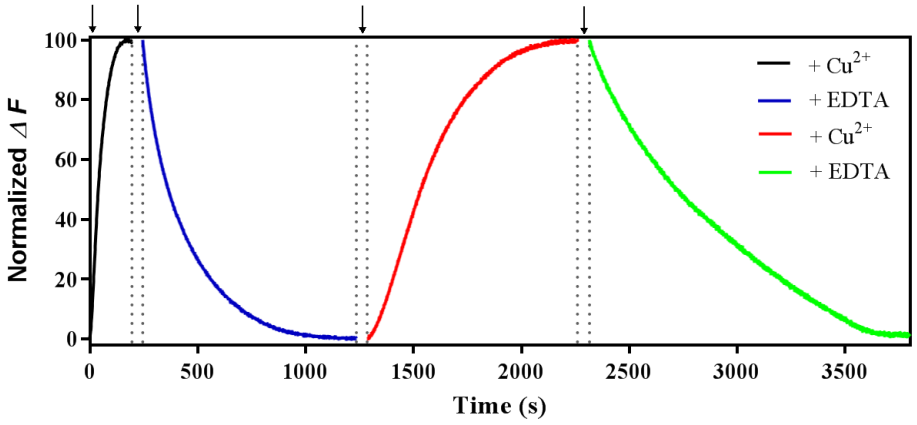

Figure S14. The kinetic behavior of reversible control by the bidirectional reporter system. In the bidirectional reporter system ($R2_Q$ and $\overline{R2}_F$), the controllable reversibility was governed by the metal-ligand complexation between State A and B as described in Figure 5d. In the first cycle, the addition of copper ion was 1 μM and the addition of EDTA was 25 μM; in the second cycle, the addition of copper ion was 25 μM and the addition of EDTA was 50 μM; After each treatment, real-time fluorescence was monitored. Concentrations for all these strands were described in the methods. The arrows represented addition of Cu^{2+} or EDTA. The reaction buffer was 20 mM Tris-HCl (pH = 8.0) with 100 mM NaCl. Initially, the fluorescence signals increased rapidly and reached the equilibrium with $t_{0.5}$ ~40 s upon the first treatment of the copper ions. When the metal chelating agent (EDTA) was added subsequently, the reaction proceeded towards the reverse direction, and the fluorescence signals were gradually quenched with $t_{0.5}$ ~120 s, which was slower than the increasing rate. Notably, with the second cycle of the copper-EDTA treatment, the fluorescence change was significantly slower than the first one, and it took a longer time to reach the equilibrium (~250 s for the second treatment of copper and ~400 s for the subsequent treatment of EDTA to achieve the 50% conversion). We speculated the competitive copper chelation between 8HQ and EDTA might contribute to the reduced efficiency of strand displacement in the system. All of these data and descriptions have been included into the revised manuscript.

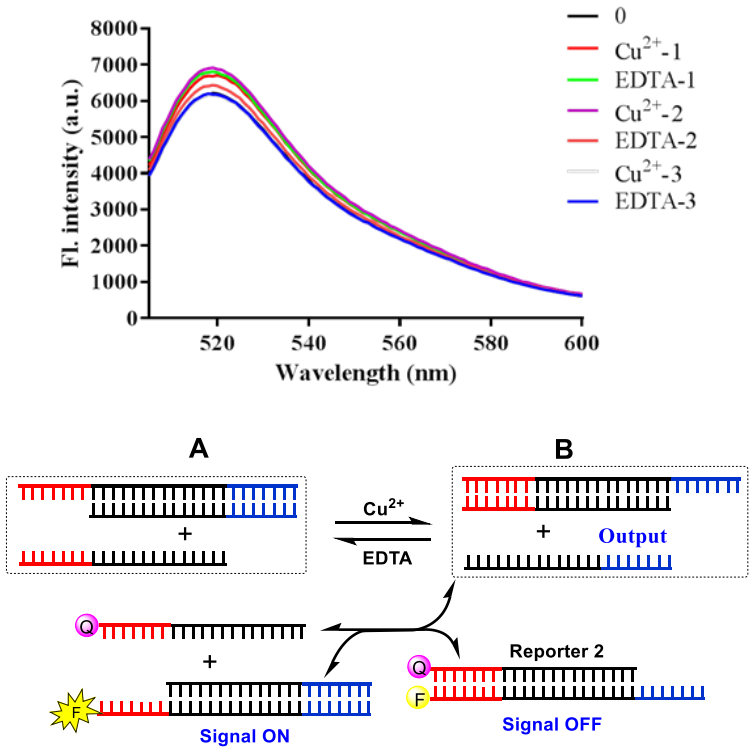

Figure S15. Fluorescence spectra of the conventional toehold-mediated strand displacement in the bidirectional reporter system. All samples underwent the same procedures as described in Figure S13. Concentrations for all these strands were described in the methods. The reaction buffer was 20 mM Tris-HCl (pH = 8.0) with 100 mM NaCl.

Supplementary Tables

Table S1. Melting temperature (T_m / ºC) and the change of the melting temperature ($\triangle T_m$ / ºC) of duplexes ($S_{L\text{-}Q}$: $\bar{S}_{L\text{-}F}$ (***S***); $S_{L\text{-}Q}$: $\bar{S}_{L\text{-}F}$ (***R***) and S_Q : $\bar{S}_F$) in the presence of different metal ions per duplex (at pH 7.5). The data of the T_m and $\triangle T_m$ were calculated from figure S3, figure 2d and figure S4.

M^{2+}	Duplex ($S_{L\text{-}Q}$: $\bar{S}_{L\text{-}F}$) (***S***)		Duplex ($S_{L\text{-}Q}$: $\bar{S}_{L\text{-}F}$) (***R***)		Duplex (S_Q : $\bar{S}_F$)	
	Tm/ ºC	△Tm/ ºC	Tm/ ºC	△Tm/ ºC	Tm/ ºC	△Tm/ ºC
No M^{2+}	55.5 ±0.2	–	55.8 ± 0.1	–	54.2 ± 0.1	–
Mg^{2+}	57.0 ± 0.1	1.5 ± 0.1	57.1 ± 0.4	1.3 ± 0.5	54.3 ± 0.3	0.1 ± 0.4
Ca^{2+}	57.0 ± 0.2	1.5 ± 0.4	57. 9 ± 1.7	2.0 ± 1.8	54.5 ± 0.2	0.3 ± 0.1
Mn^{2+}	57.0 ± 0.2	1.6 ± 0.2	58.3 ± 0.3	2.4 ± 0.4	54.3 ± 0.1	0.1 ± 0.2
Ni^{2+}	63.3 ± 0.1	7.8 ± 0.3	63.7 ± 0.3	7.9 ± 0.2	54.1 ± 0.1	-0.1 ± 0.1
Cu^{2+}	71.5 ± 0.1	16.0 ± 0.2	71.2 ± 0.5	15.4 ± 0.6	54.0 ± 0.2	-0.2 ± 0.1
Zn^{2+}	60.8 ± 0.1	5.3 ± 0.1	63.3 ± 0.1	7.5 ± 0.1	54.4 ± 0.3	0.2 ± 0.2
Pb^{2+}	59.0 ± 0.1	3.5 ± 0.1	60.9 ± 0.1	5.5 ± 0.1	54.1 ± 0.3	-0.1 ± 0.4

Table S2. Sequences of **8HQ**-modified DNA strands used in this study.[a]

DNA strands	Sequences	Calcd.	Found[b]
S_L (***S***) [c]	5' - **8HQ (*S*)** GAG ACT ACT GGC TAT GGT GCT- 3'	6801.2	6802.8
$\bar{S}_L$ (***S***)	5'- AG CAC CAT AGC CAG TAG TCT C **8HQ (*S*)** -3'	6699.2	6700.2
$\bar{S}_{L\text{-}F}$ (***S***)	5'（**FAM**）- AG CAC CAT AGC CAG TAG TCT C **8HQ (*S*)** - 3'	7236.7	7235.3
$S_{L\text{-}Q}$ (***S***)	5' - **8HQ (*S*)** GAG ACT ACT GGC TAT GGT GCT - (**BHQ_1**) 3'	7355.7	7354.6
$\bar{S}_{LP1}$ (***S***)	5'- AG CAC CAT AGC CAG TAG TCT **G 8HQ (*S*)**- 3	6739.2	6737.7
$\bar{S}_{LP4}$ (***S***)	5'- AG CAC CAT AGC CAG TAG **C**CT C **8HQ (*S*)** - 3'	6684.2	6683.0
$\bar{S}_{LP11}$ (***S***)	5'- AG CAC CAT AG**G** CAG TAG TCT C **8HQ (*S*)** - 3'	6739.2	6738.0
$\bar{S}_{LP18}$ (***S***)	5'- AG C**C**C CAT AGC CAG TAG TCT C **8HQ (*S*)** - 3'	6675.2	6673.8
S_{LT} (***S***)	5'- **8HQ (*S*)** GAG ACT ACT GGC TAT GGT GCT **GAA CTC T**-3'	8943.6	8942.3
S_L (***R***) [d]	5'- **8HQ (*R*)** GAG ACT ACT GGC TAT GGT GCT -3'	6801.2	6801.4
$\bar{S}_L$ (***R***)	5'- AG CAC CAT AGC CAG TAG TCT C **8HQ (*R*)** - 3'	6699.2	6699.4
$S_{L\text{-}Q}$ (***R***)	5'- **8HQ (*R*)** GAG ACT ACT GGC TAT GGT GCT-(**BHQ_1**)3'	7355.7	7355.9
$\bar{S}_{L\text{-}F}$ (***R***)	5'（**FAM**）- AG CAC CAT AGC CAG TAG TCT C **8HQ (*R*)** - 3'	7236.7	7236.3

[a] All these sequences were prepared according to the procedure described in the synthesis of 8HQ-modified DNA sequences；[b] Mass observed in MALDI-TOF MS analysis; [c] ***S*** refers to the ***S*** configuration; [d] ***R*** refers to the ***R*** configuration.

Table S3. Unmodified DNA strands used in this study.

DNA strands	Sequences
S_1	5'- GAG ACT ACT GGC TAT GGT GCT -3'
$\bar{S}_1$	5'- AG CAC CAT AGC CAG TAG TCT C- 3'
$\bar{S}_F$	5'（**FAM**）-AG CAC CAT AGC CAG TAG TCT C- 3'
S_Q	5'- GAG ACT ACT GGC TAT GGT GCT -(**BHQ$_1$**)3'
$\bar{S}_{F\text{-}A}$	5'（**FAM**）-AG CAC CAT AGC CAG TAG TCT C **A**- 3
$S_{Q\text{-}T}$	5' - **T** GAG ACT ACT GGC TAT GGT GCT - (**BHQ$_1$**)- 3'
$S_{T\text{-}Q}$	5'-**CTG ATA C** GAG ACT ACT GGC TAT GGT GCT（**BHQ$_1$**）-3'
$\bar{S}_T$	5'- AGC ACC ATA GCC AGT AGT CTC **GTA TCA G**-3'
$\bar{S}_{T1}$	5'- **AGA GTT C**AG CAC CAT AGC CAG TAG TCT C -3'
R1	5'- AGC ACC ATA GCC AGT AGT CTC –3'
$R1_Q$	5'- AGC ACC ATA GCC AGT AGT CTC –(**BHQ$_1$**)3'
$\overline{R1}_F$	5'（**FAM**）-GAG ACT ACT GGC TAT GGT GCT **GAA CTC T** -3'
S_{T2}	5'-**CTG ATA C** GAG ACT ACT GGC TAT GGT GCT **GAA CTC T** -3'
$\overline{R2}_F$	5'-(**FAM**) **AGG ACT T** GAG ACT ACT GGC TAT GGT GCT **GAA CTC T**-3'
$R2_Q$	5'-AGC ACC ATA GCC AGT AGT CTC **AAG TCC T**（**BHQ$_1$**）-3'

ESI spectra of 8HQ-modified DNA sequences

Strands with the *S*-configuration ligand

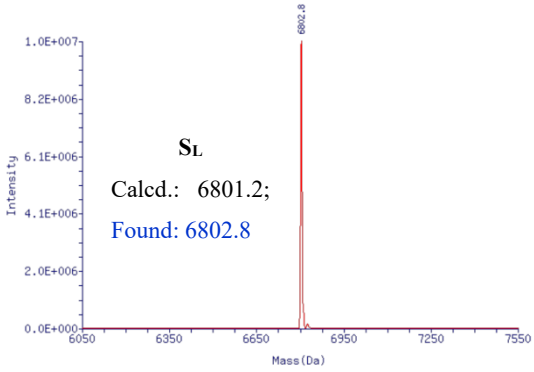

S_L

Calcd.: 6801.2;

Found: 6802.8

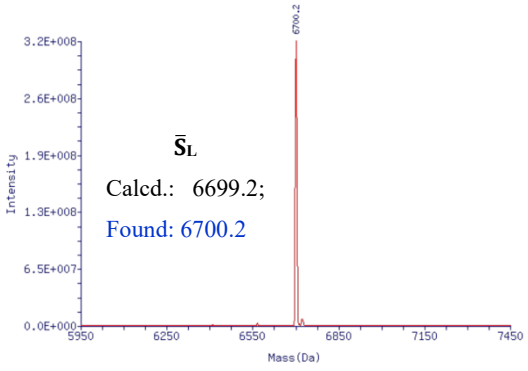

$\bar{S}_L$

Calcd.: 6699.2;

Found: 6700.2

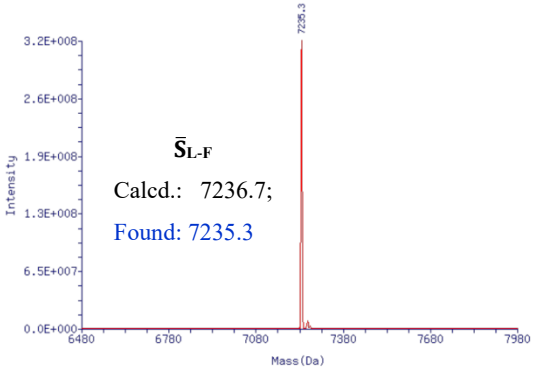

$\bar{S}_{L\text{-}F}$

Calcd.: 7236.7;

Found: 7235.3

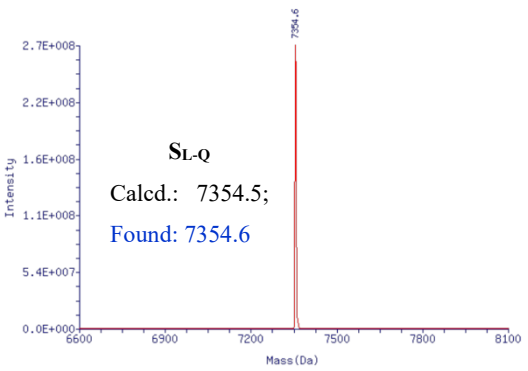

$S_{L\text{-}Q}$

Calcd.: 7354.5;

Found: 7354.6

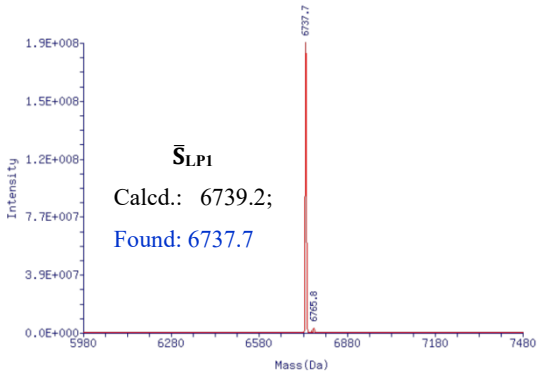

$\bar{S}_{LP1}$

Calcd.: 6739.2;

Found: 6737.7

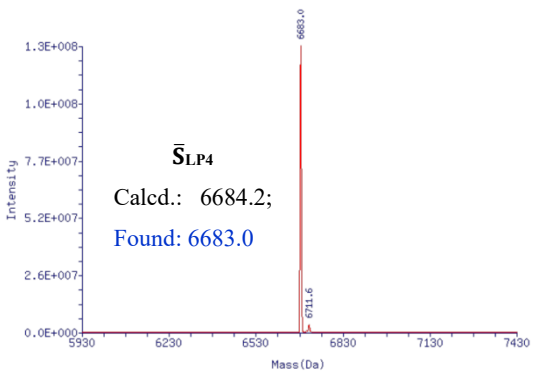

$\bar{S}_{LP4}$

Calcd.: 6684.2;

Found: 6683.0

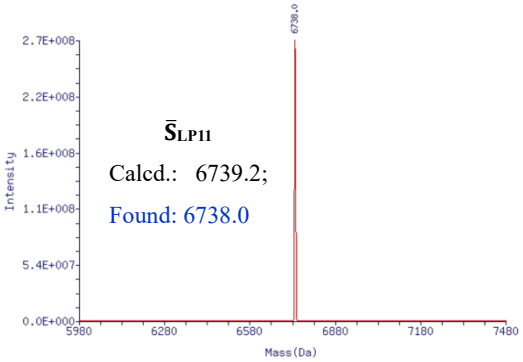

$\bar{S}_{LP11}$

Calcd.: 6739.2;

Found: 6738.0

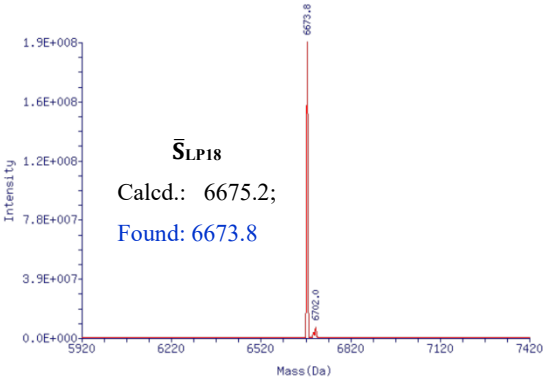

$\bar{S}_{LP18}$

Calcd.: 6675.2;

Found: 6673.8

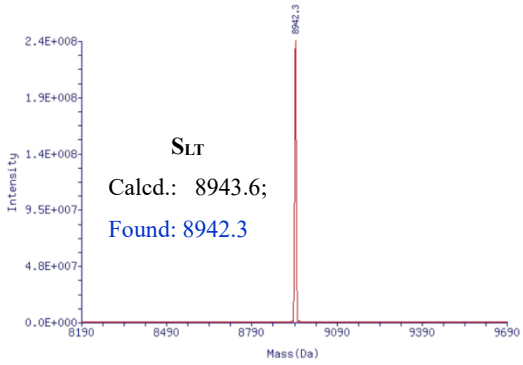

S_{LT}

Calcd.: 8943.6;

Found: 8942.3

Strands with the *R*-configuration ligand

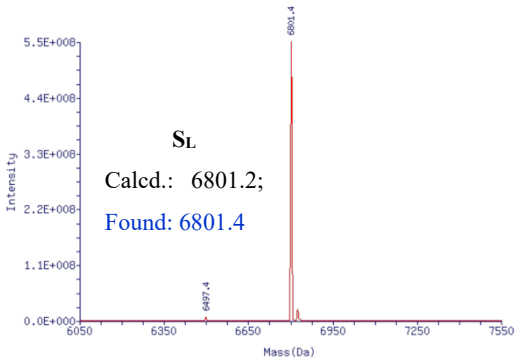

S_L

Calcd.: 6801.2;

Found: 6801.4

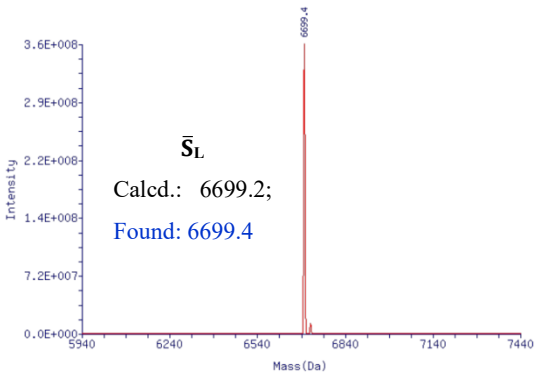

$\bar{S}_L$

Calcd.: 6699.2;

Found: 6699.4

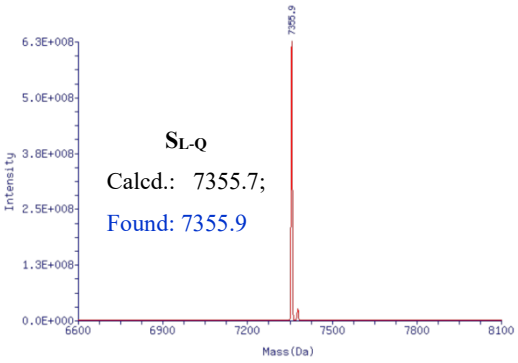

$S_{L\text{-}Q}$

Calcd.: 7355.7;

Found: 7355.9

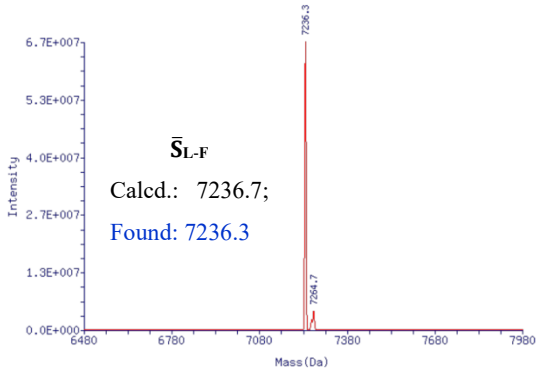

$\bar{S}_{L\text{-}F}$

Calcd.: 7236.7;

Found: 7236.3

The NMR spectra of synthetic compounds

^{1}H NMR spectrum （Compound 2）

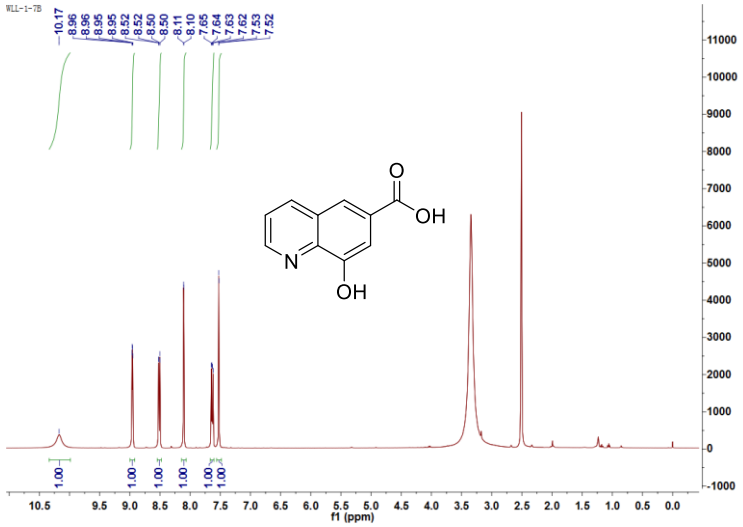

C^{13} NMR spectrum （Compound 2）

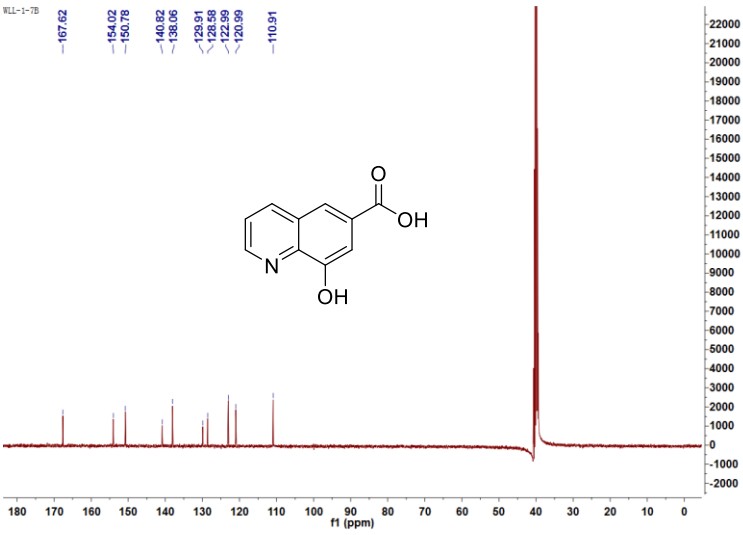

MS spectrum （Compound 2）

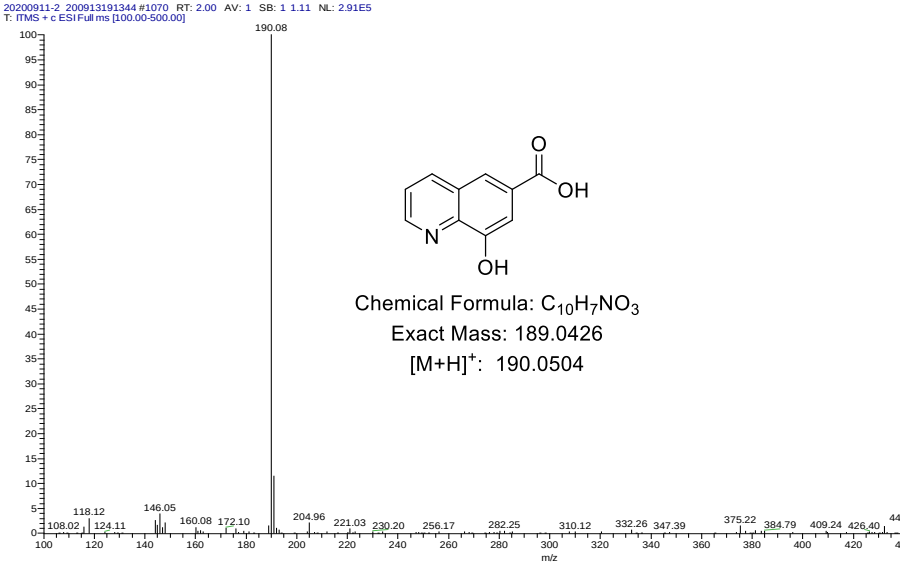

^{1}H NMR spectrum （Compound 3）

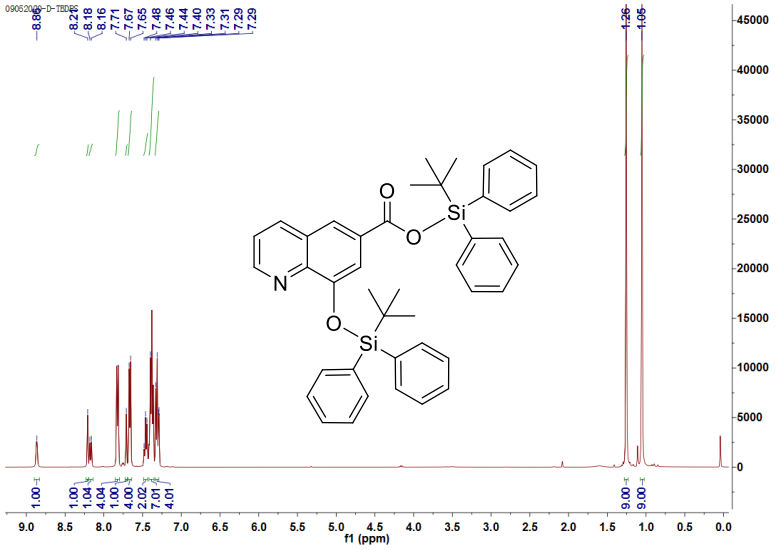

C^{13} NMR spectrum （Compound 3）

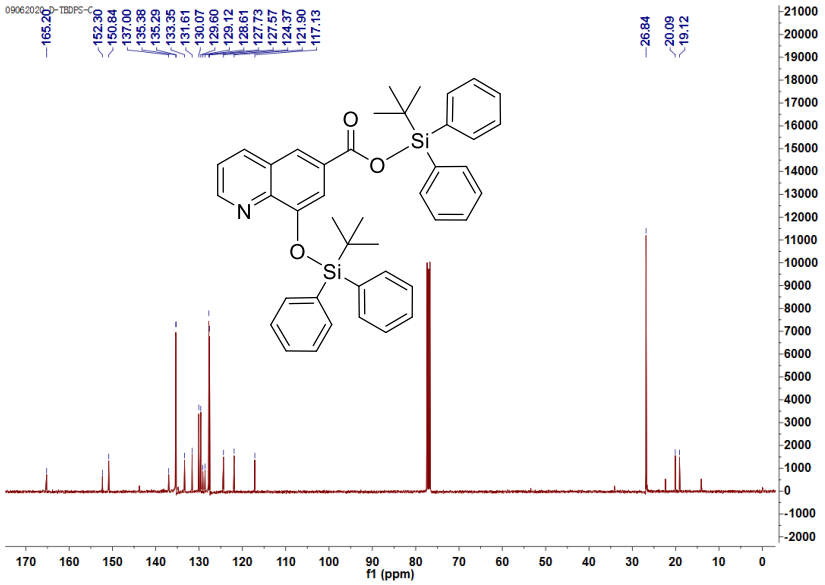

MS spectrum （Compound 3）

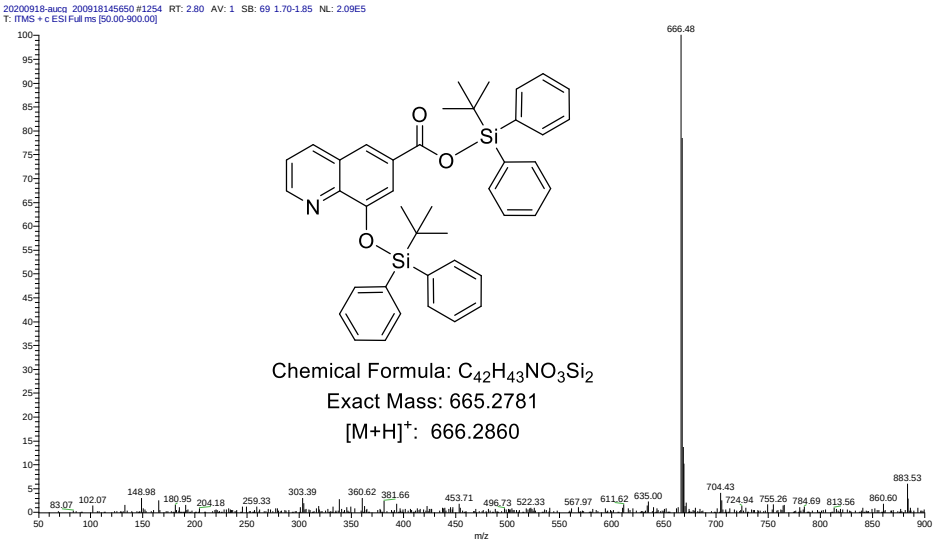

^{1}H NMR spectrum （Compound 4）

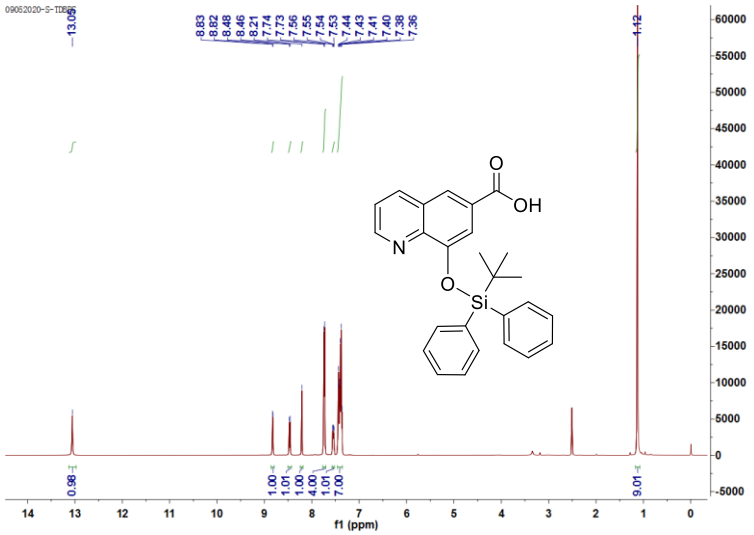

C^{13} NMR spectrum （Compound 4）

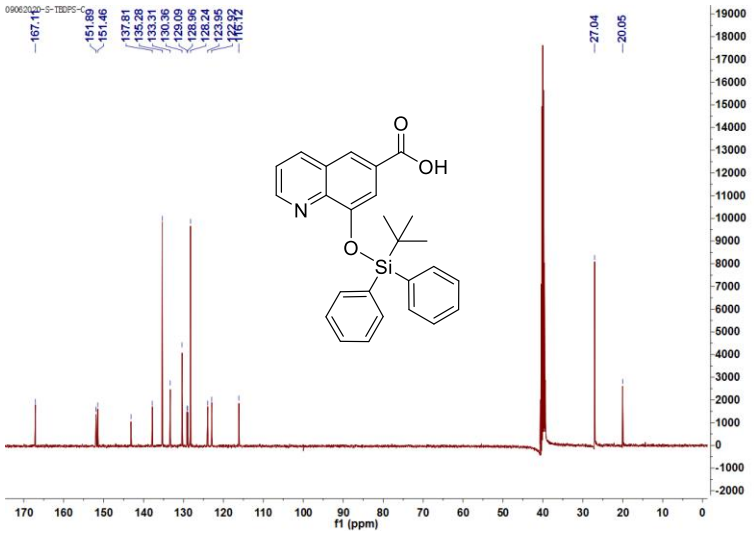

MS spectrum （Compound 4）

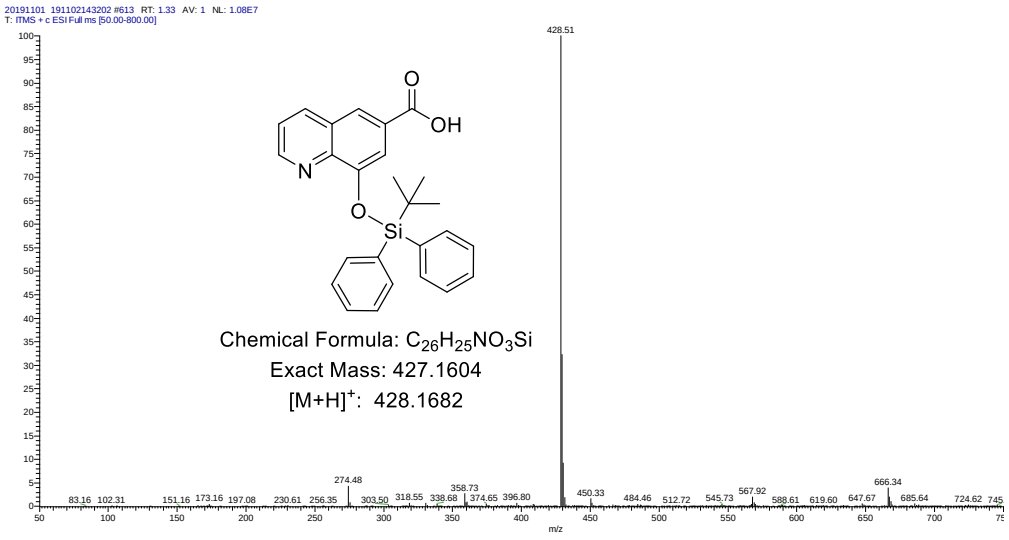

^{1}H NMR spectrum （Compound 5a）

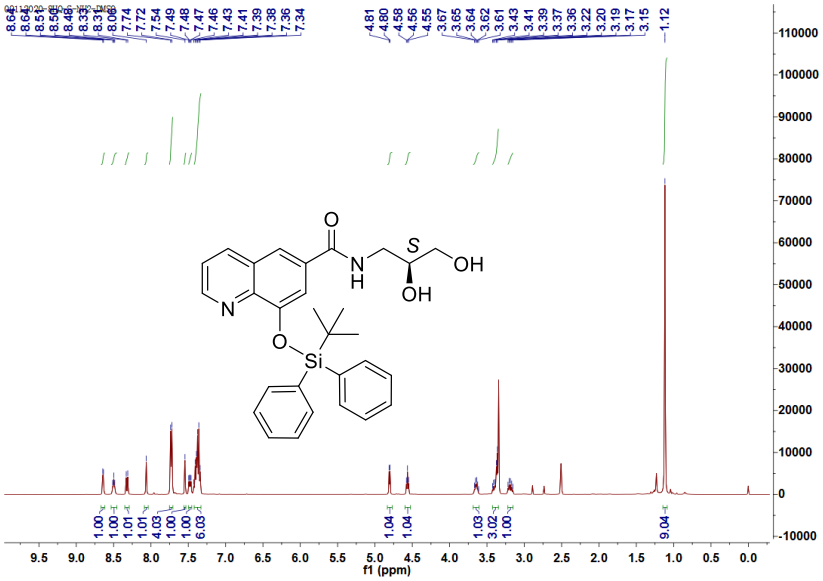

C^{13} NMR spectrum （Compound 5a）

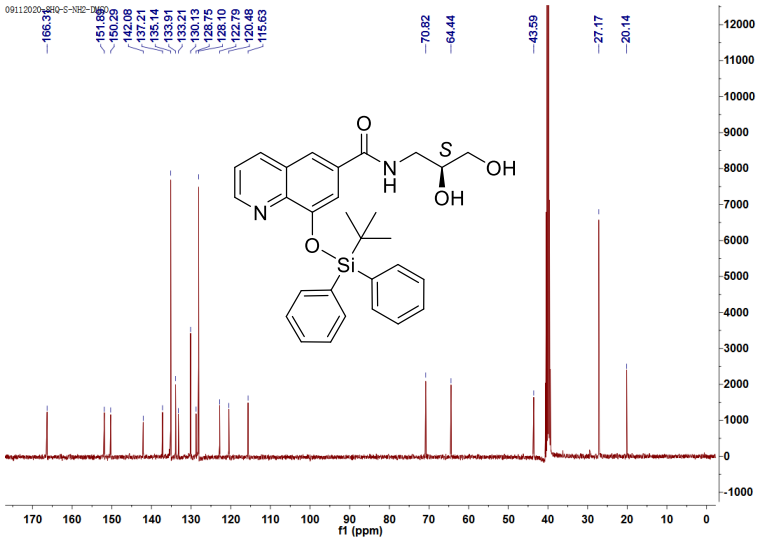

MS spectrum （Compound 5a）

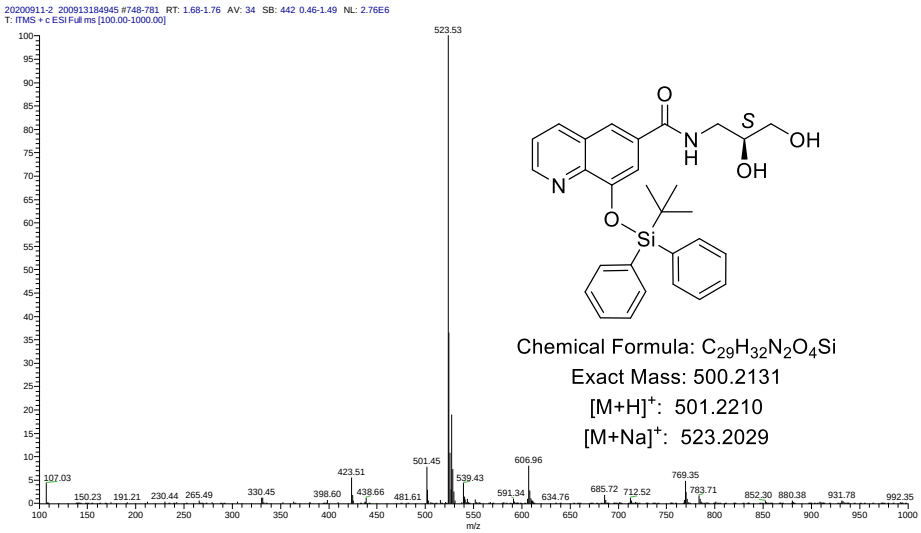

^{1}H NMR spectrum （Compound 5b）

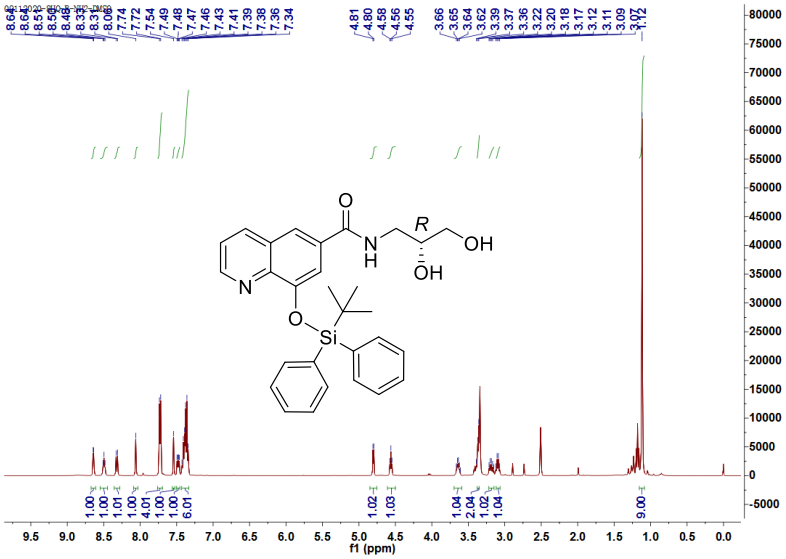

C^{13} NMR spectrum （Compound 5b）

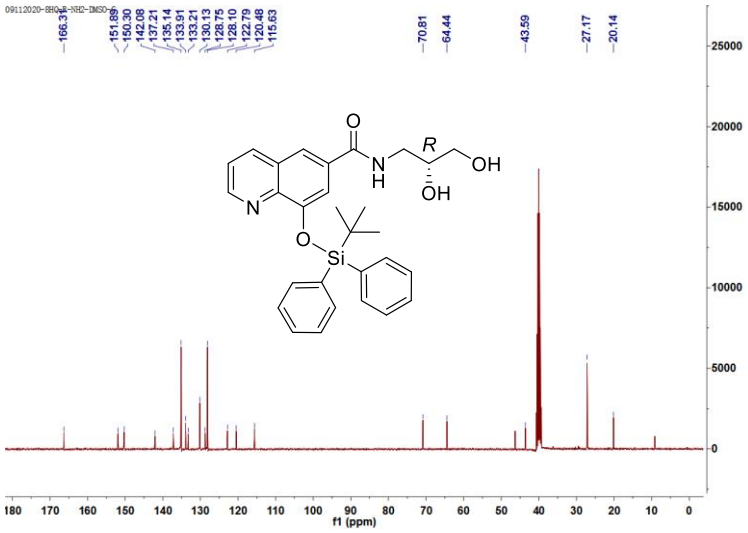

MS spectrum （Compound 5b）

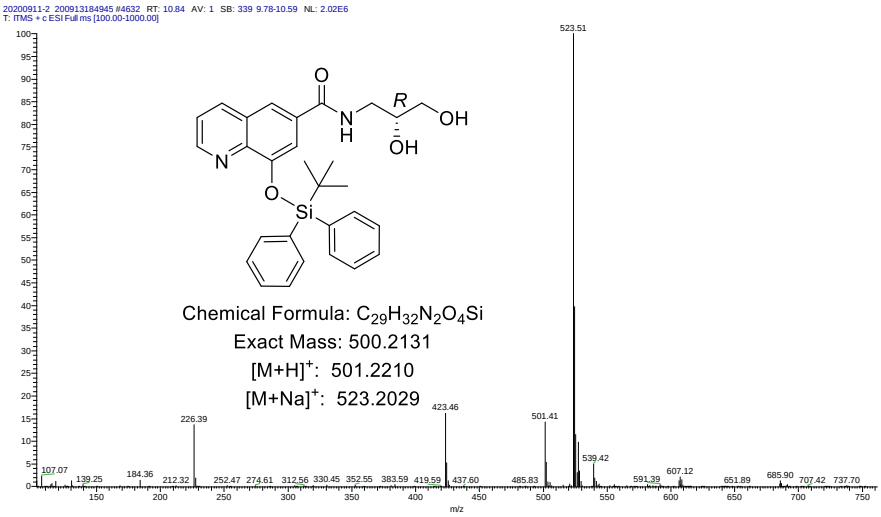

^{1}H NMR spectrum （Compound 6a）

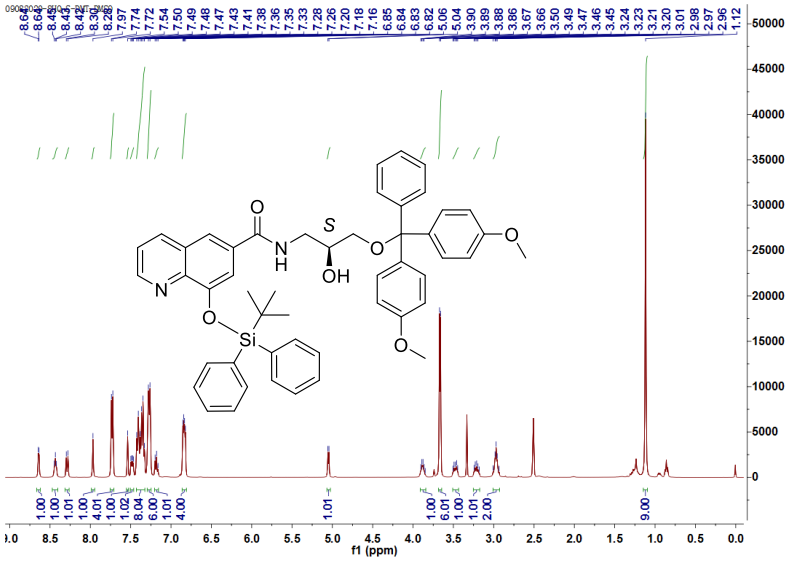

C^{13} NMR spectrum （Compound 6a）

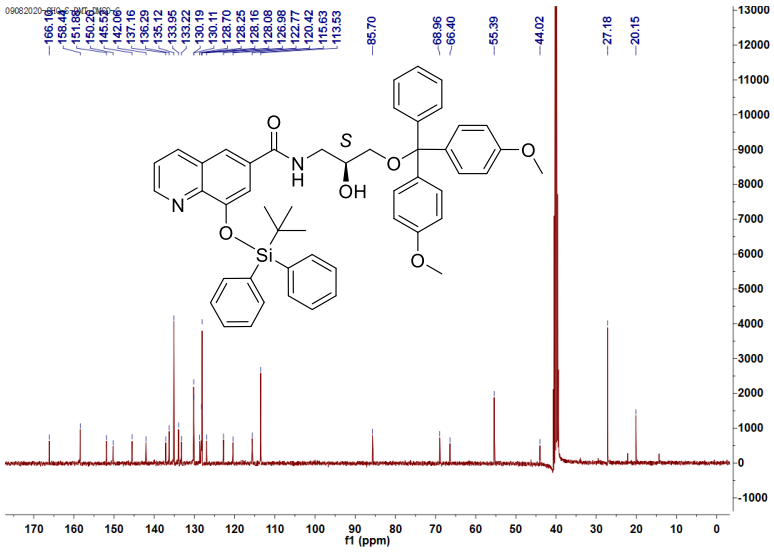

MS spectrum （Compound 6a）

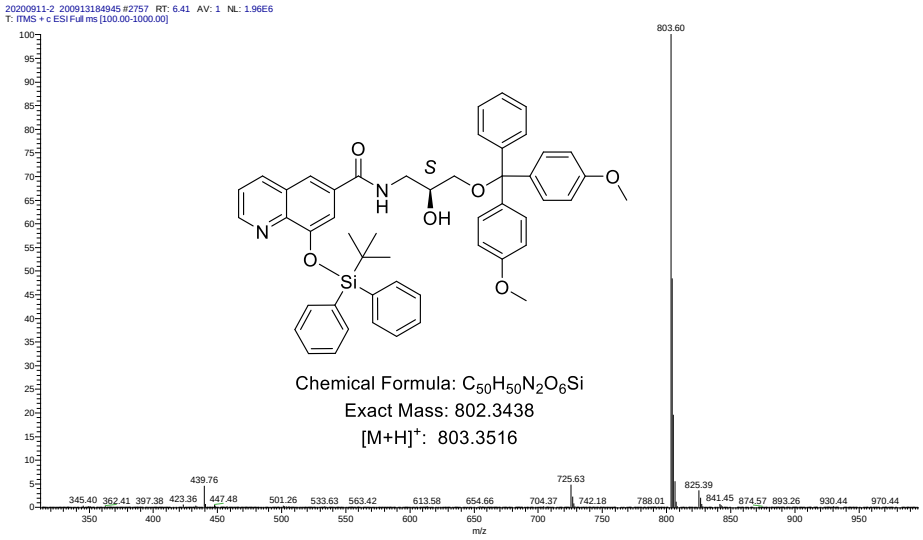

^{1}H NMR spectrum （Compound 6b）

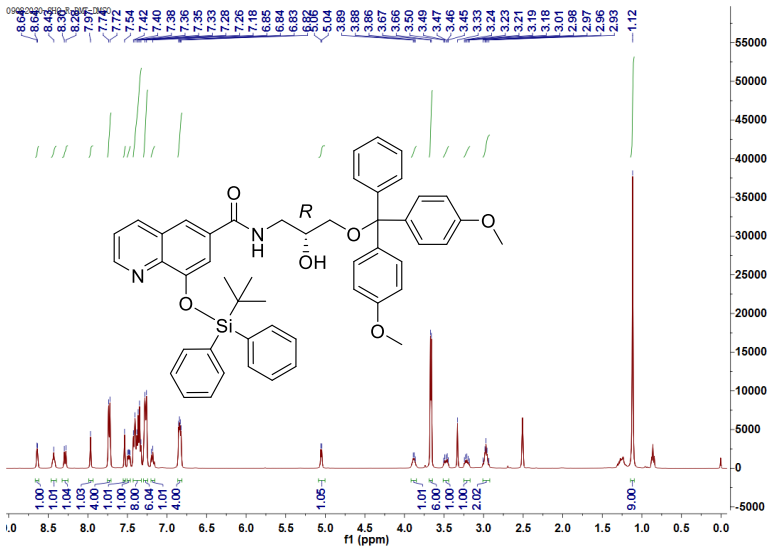

C^{13} NMR spectrum （Compound 6b）

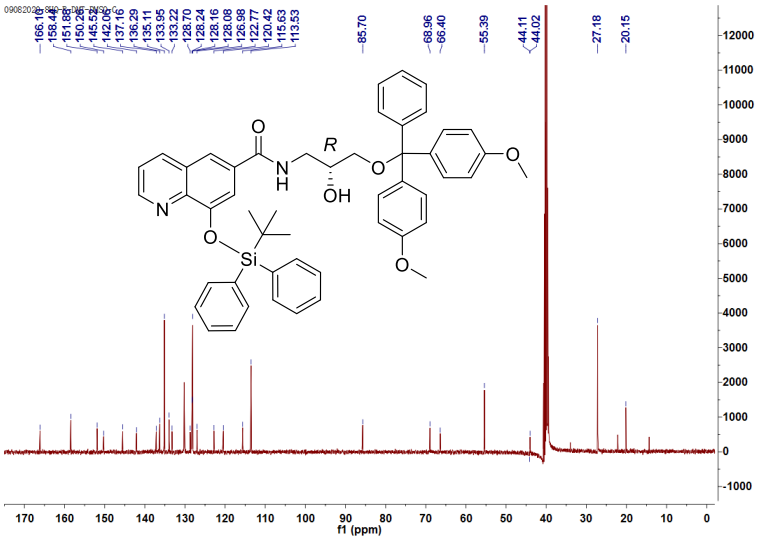

MS spectrum （Compound 6b）

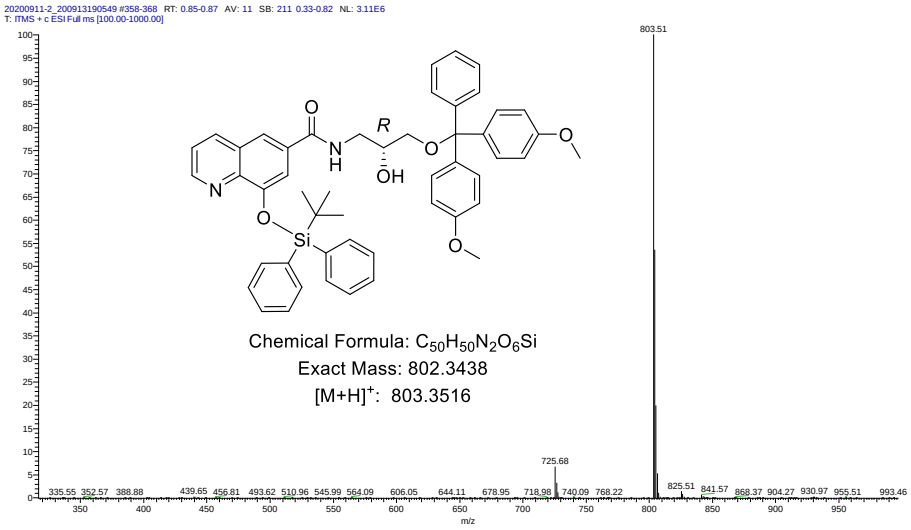

^{1}H NMR spectrum （Compound 7a）

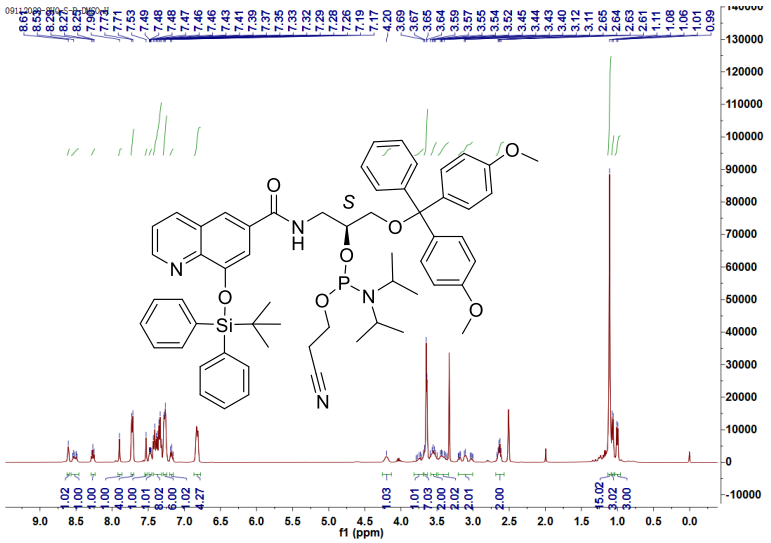

C^{13} NMR spectrum （Compound 7a）

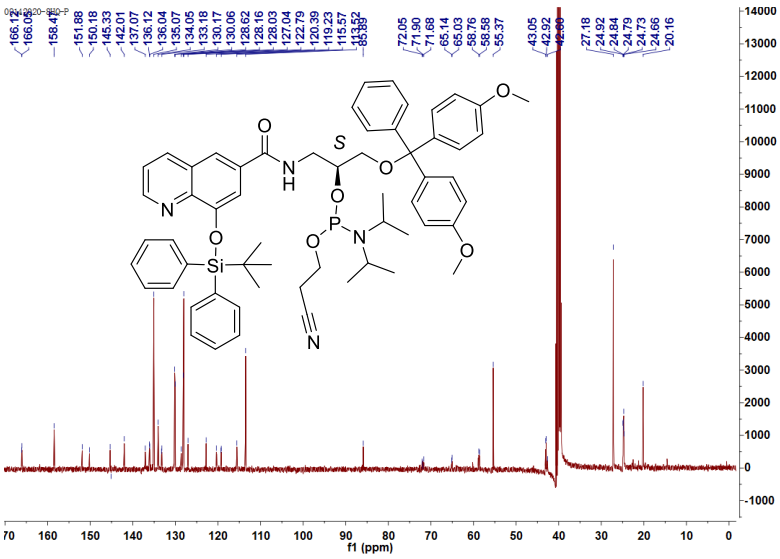

^{31}P NMR （Compound 7a）

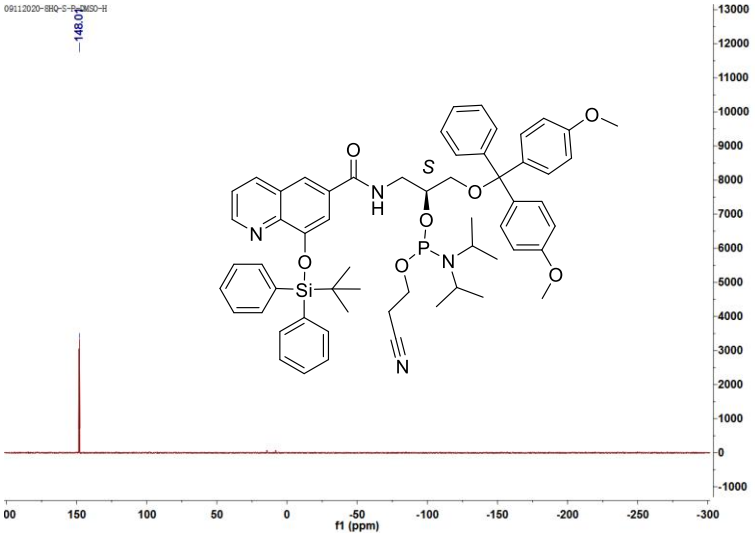

MS spectrum （Compound 7a）

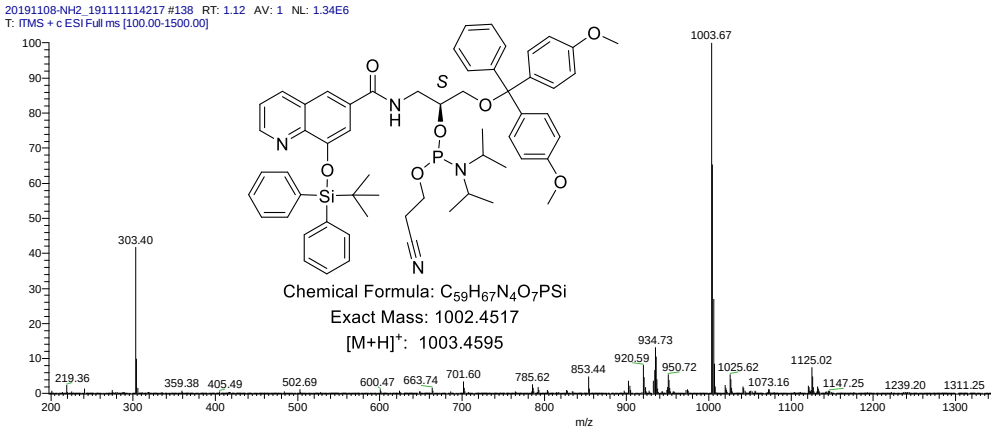

^{1}H NMR spectrum （Compound 7b）

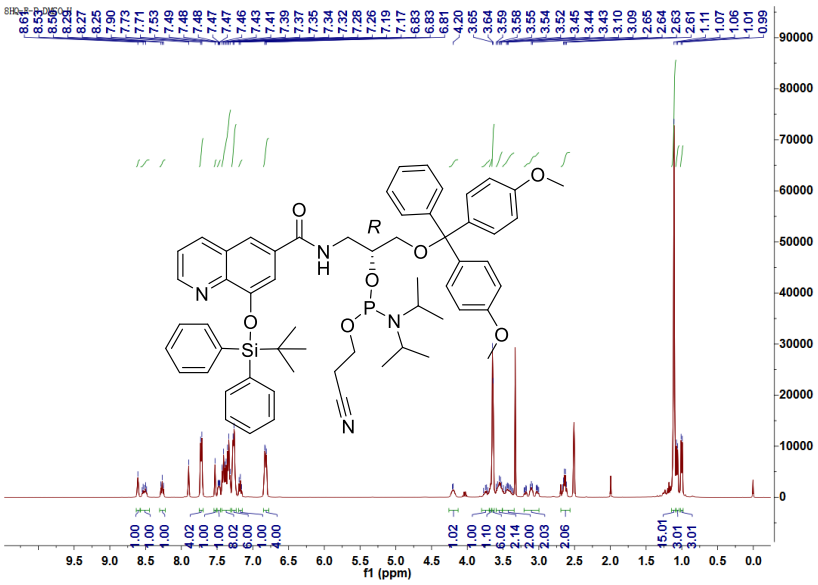

C^{13} NMR spectrum （Compound 7b）

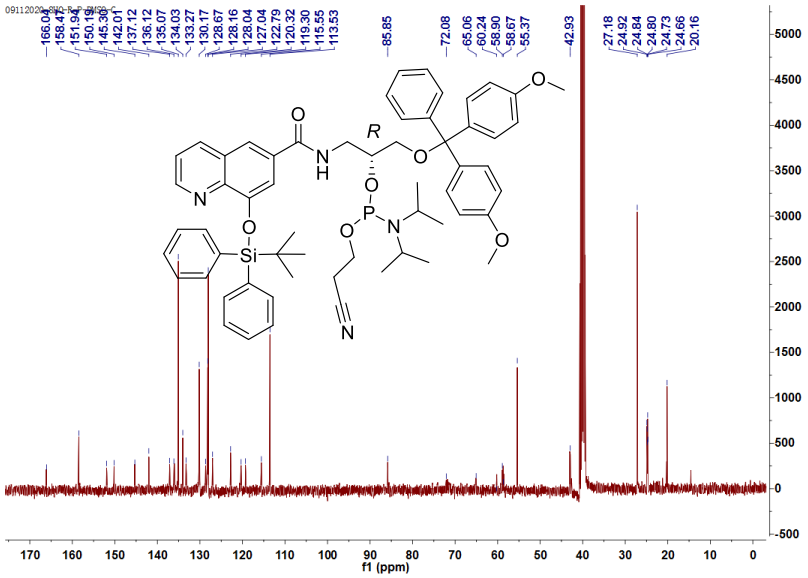

^{31}P NMR spectrum （Compound 7b）

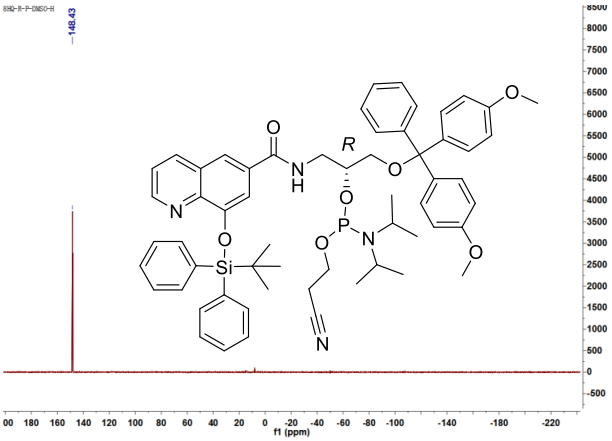

MS spectrum （Compound 7b）

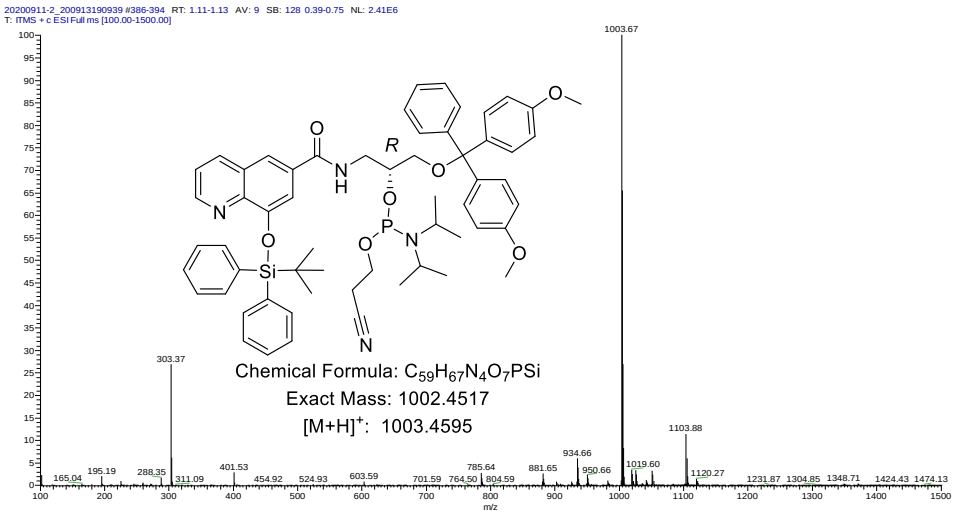

Reference

[1] I. Sosic, B. Mirkovic, K. Arenz, B. Štefane, J. Kos, S. Gobec, *J. Med. Chem.*, **2013**, 56, 521−533.